INTERNATIONAL JOURNAL OF ROBUST AND NONLINEAR CONTROL
Int. J. Robust. Nonlinear Control 2010; **00**:1–29
Published online in Wiley InterScience (www.interscience.wiley.com). DOI: 10.1002/rnc

Fault-tolerant Control of Discrete-time LPV systems using Virtual Actuators and Sensors

S. Mojtaba Tabatabaeipour[1]*, Jakob Stoustrup[2], and Thomas Bak[2]

[1]*Automation and Control, Department of Electrical Engineering, Technical University of Denmark, Elektrovej, 2800 Kgs. Lyngby, Denmark,* [2]*Automation and Control, Department of Electronic Systems,Aalborg University, Fr. Bajers Vej C7, 9200 Aalborg, Denmark*

SUMMARY

This paper proposes a new fault-tolerant control (FTC) method for discrete-time linear parameter varying (LPV) systems using a reconfiguration block. The basic idea of the method is to achieve the FTC goal without re-designing the nominal controller by inserting a reconfiguration block between the plant and the nominal controller. The reconfiguration block is realized by an LPV virtual actuator and an LPV virtual sensor. Its goal is to transform the signals from the faulty system such that its behavior is similar to that of the nominal system from the viewpoint of the controller. Furthermore, it transforms the output of the controller for the faulty system such that the stability and performance goals are preserved. Input-to-state stabilizing LPV gains of the virtual actuator and sensor are obtained by solving linear matrix inequalities (LMIs). We show that separate design of these gains guarantees the input-to-state stability (ISS) of the closed-loop reconfigured system. Moreover, we obtain performances in terms of the ISS gains for the virtual actuator, the virtual sensor and their interconnection. Minimizing these performances is formulated as convex optimization problems subject to LMI constraints. Finally, the effectiveness of the method is demonstrated via a numerical example and stator current control of an induction motor.

Received . . .

KEY WORDS: Fault-tolerant control, reconfigurable control, linear parameter varying systems, discrete-time systems

1. INTRODUCTION

There is an increasing demand for safety, reliability and performance of modern industrial systems. A fault in the system might deteriorate the performance of the system or lead to the loss of the system functionality or stability. In some instances, it might result in hazardous events. Therefore, it is very important to design control systems that can tolerate occurrence of some faults during the operation while guaranteeing stability and functionality of the system and maintaining an acceptable performance. Such controllers are called fault-tolerant. The area of fault-tolerant control (FTC) has attracted a lot of attentions is the past two decades, see review papers [1], [2], [3] and books [4] and [5].

Broadly speaking, FTC systems are divided into two categories: passive (PFTC) and active (AFTC). In PFTC, the FTC system does not react to the occurrence of a fault in the sense that the structure and parameters of the controller are pre-designed and fixed such that it can tolerate a set of faults without any change in the controller. This means that the fault tolerant controller provides a common solution to the problem of control design for the normal system as well as the faulty system.

*Correspondence to: setaba@elektro.dtu.dk

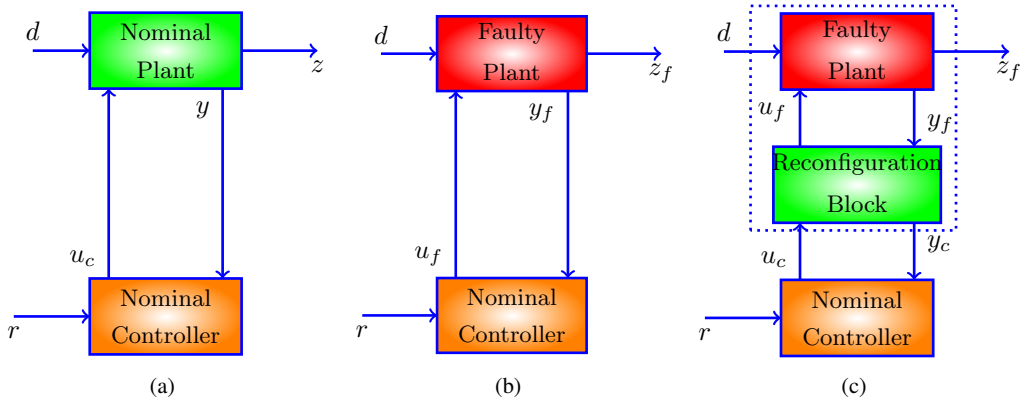

Figure 1. Fault-tolerant control using a reconfiguration block: (a) nominal loop, (b) faulty plant with nominal controller, (c) reconfigured plant with nominal controller

Therefore, the PFTC solution is usually a conservative solution. Moreover, when some severe faults are taken into account, a common solution may not always exist and if it exists, it usually yields a low performance. On the other hand in AFTC, the controller reacts to the occurrence of faults and changes the parameters and/or the structure of the controller. A fault detection and estimation module is used to detect and estimate the fault when it occurs. Then, based on the information about the occurred fault, a supervisory controller changes the control law or the structure of the controller, in the case of severe faults, such that the faulty system with the new controller is stable and provides an acceptable performance. AFTC can usually provide a better performance because it changes or modifies the controller based on the characterizations of the occurred fault.

In most of the AFTC methods developed in the literature, a specific controller is designed for each faulty case. When the fault is detected and estimated, the controller is switched to the controller designed specifically for the system subject to the detected fault. In this paper, the idea is to keep the nominal control in the loop and design a reconfiguration block, which is inserted between the faulty system and nominal system such that the overall stability of the closed-loop is preserved. This idea is depicted in Figure 1. The idea of control reconfiguration using a virtual sensor and actuator was first proposed in [6] and later in [7] for linear systems. The goal of the reconfiguration block is to transform the output of the faulty plant to an appropriate signal such that from the nominal controller's viewpoint its behavior is similar to that of the nominal plant. The reconfiguration block is realized respectively by a virtual sensor, a virtual actuator or a series connection of both a virtual sensor and a virtual actuator in case of a sensor fault, an actuator fault, and a simultaneous sensor and actuator fault.

The main advantage of the proposed approach is in practical applications where another supplier provides the controller and due to the complexity of the control systems as such as well as insurance or legal reasons, we do not have access to or information about the inside of the controller box. The proposed method helps us to achieve fault tolerance in these situations without any change to the nominal controller.

A control reconfiguration method using an observer for sensor faults and its dual for actuator faults based on loop transfer recovery design is proposed in [6]. In [7] virtual actuators and virtual sensors for linear systems are investigated. In [8] it is shown that control reconfiguration of a linear system after an actuator fault is equivalent to disturbance decoupling. A fault-tolerant control method using virtual actuator combined with set-separation method fault detection for linear systems subject to actuator faults is proposed in [9]. Control reconfiguration using virtual actuators and sensors for piecewise affine systems and Hammerstein-Wiener systems are proposed in [10], [11], [12] and [13]. FTC for Lur'e systems with Lipschitz continuous nonlinearity subject to actuator fault using a virtual actuator is presented in [14] where it is assumed that the state of the faulty

DOI: 10.1002/rnc

system is measurable. FTC for a system with additive Lipschitz nonlinearity subject to actuator faults using a virtual actuator is presented in [15].

[16] proposes using virtual sensors for fault tolerant control of polytopic LPV systems subject to sensor faults. The structure of the nominal controller is assumed to be known. It is assumed that the nominal controller consists of a state feedback controller combined with an LPV observer. When a sensor fault occurs, a virtual sensor is used to hide the fault. In [17] an FTC method using virtual sensor for polytopic LPV systems subject to sensor faults is proposed where the fault is detected using robust fault detection based on invariant-set methods. In a previous work [18], we considered the problem of control reconfiguration for continuous-time LPV systems where both sensor and actuator faults were considered and only input-to-state stability (ISS) properties of the reconfigured system were investigated.

In this paper, we consider the problem for discrete-time LPV system. We address both actuator and sensor faults. We do not assume any specific structure for the nominal controller. It is only assumed that the nominal controller is designed such that the nominal closed loop system is input-to-state stable (ISS). Then, we show that if we design the virtual actuators and the virtual sensor separately such that each of them is ISS, we can guarantee that the closed loop reconfigured system is also ISS. We derive sufficient conditions in terms of LMIs for designing input-to-state stabilizing virtual actuator and sensors. We also obtain performance in terms of ISS gains for the virtual actuator and virtual sensor as well as the their interconnection i.e the reconfiguration block. We formulate minimizing the performance of the virtual actuator and virtual sensor as a convex optimization problem with LMI constraints. Finally, we obtain the performance of the reconfiguration block in terms of ISS gains of the virtual actuator and the virtual sensor.

In contrast to [16] and [17], we consider both actuator and sensor faults. Also, we do not make any assumption about the structure of the controller. This is important in practical cases where another supplier provides the controller and we do not have information about the structure or the parameters of the controller. We prove the stability properties of the systems in the ISS paradigm. Moreover, we consider the performance in terms of ISS gains and we discuss how to optimize the performance. Stability in the ISS sense turns out to be very practical since it is a global notion and it implies robust stability as showed in [19].

This paper is organized as follows. In Section 2, preliminaries and some basic definitions are given. In Section 3 LPV systems and faults are introduced and the reconfiguration problem for LPV systems is defined. Control reconfiguration of LPV systems using a virtual actuator and a virtual sensor is discussed in Section 4. In Section 5, the method is demonstrated on a numerical example as well as on stator current control of an induction motor. Finally, conclusions are given in Section 6.

2. PRELIMINARIES

The field of real numbers, the set of nonnegative reals and the set of nonnegative integers are respectively denoted by $\mathbb{R}, \mathbb{R}_{\geq 0}, \mathbb{N}$. For any $x \in \mathbb{R}^n$, x^T stands for its transpose and $\|x\| = \sqrt{x^T x}$ denotes its Euclidean norm. Also, the i-th entry of x is denoted by x^i. The infinity norm of x denoted by $\|x\|_\infty$ is given by $\max_i |x|$. Given a sequence $\{v(k)\}_{k\in\mathbb{N}}$, its supremum norm i.e $\sup_{k\in\mathbb{N}}\|v(k)\|$ is denoted by $\|v\|_\infty$.

A function $\gamma : \mathbb{R}_{\geq 0} \to \mathbb{R}_{\geq 0}$ is a class $\mathcal{K}$ function if it is continuous, strictly increasing, and $\gamma(0) = 0$. γ is a class $\mathcal{K}_\infty$ function if it is a class $\mathcal{K}$ function and also it satisfies $\gamma(s) \to \infty$ as $s \to \infty$. A function β is a class $\mathcal{KL}$ function if for each fixed $k \in \mathbb{R}_{\geq}0$, the function $\beta(\cdot, k) \in \mathcal{K}$, and for each fixed $s \in \mathbb{R}_{\geq 0}$, the function $\beta(s, \cdot)$ is decreasing and $\beta(s,k) \to 0$ as $k \to \infty$. In the following we recall definitions of input-to-state stability for nonlinear discrete-time system [20]. Consider the following nonlinear discrete-time system:

$$\begin{cases} x(k+1) = f(x(k), v(k)), \\ y(k) = h(x(k)), \end{cases} \tag{1}$$

DOI: 10.1002/rnc

where $x(k) \in \mathbb{R}^n$ is the state, and $v(k) \in \mathbb{R}^d$ is an unknown input disturbance.

Definition 1
The zero-input nonlinear system (1) i.e. $x(k+1) = f(x(k),0))$ is globally asymptotically stable (GAS) if there exist a $\mathscr{K}\mathscr{L}-$function β such that for each initial condition $x(0) \in \mathbb{R}^n$, all solutions of the system satisfy:

$$\|x(k)\| \leq \beta(\|x(0)\|,k). \tag{2}$$

In case β can be chosen as $\beta(s,k) = ds\lambda^k$ for some $d \geq 0$ and $0 \leq \lambda < 1$, then the system (1) is called globally exponentially stable (GES).

Definition 2
The nonlinear system (1) is called input-to-state stable (ISS) with respect to the input v if there exists $\mathscr{K}\mathscr{L}$ function β and a class $\mathscr{K}$ function γ such that for each initial condition $x(0) \in \mathbb{R}^n$ and all inputs $\{v(k)\}_{k\in\mathbb{N}}$, all solutions of the system satisfy:

$$\|x(k)\| \leq \beta(\|x(0)\|,k) + \gamma(\|v\|_\infty). \tag{3}$$

The function γ is called the ISS gain of (1) with respect to the input v. When $v(k)$ is zero then (3) reduces to $\|x(k)\| \leq \beta(\|x(0)\|,k)$ which implies that zero-input system $x(k+1) = f(x(k),0)$ is asymptotically stable. Also, $\beta(\|x(0)\|,k) \to 0$ as $k \to \infty$. Intuitively speaking, this means that for large k the size of the state is bounded by the amplitude of the input (possibly in a nonlinear way). At the other hand, for small k the term $\beta(\|x(0)\|,k)$ may dominate $\gamma(\|v\|_\infty)$ which determines the transient behavior of the system [21].

Definition 3
The nonlinear system (1) is called Input-to-output stable (IOS) with respect to the input v if there exist a $\mathscr{K}\mathscr{L}$ function β and a class $\mathscr{K}$ function γ such that:

$$\|y(k)\| \leq \beta(\|x(0)\|,k) + \gamma(\|v\|_\infty). \tag{4}$$

Theorem 1
[20], [22] Let $V : \mathbb{R}^n \to \mathbb{R}_{\geq 0}$ be a continuous function. If there exist a class $\mathscr{K}_\infty$ functions α_1 and α_2 such that:

$$\alpha_1(\|x\|) \leq V(x) \leq \alpha_2(\|x\|), \forall x \in \mathbb{R}^n \tag{5}$$

and if there exist a class $\mathscr{K}_\infty$ function α_3 and a $\mathscr{K}$ function σ such that

$$V(f(x,v)) - V(x) \leq -\alpha_3(\|x\|) + \sigma(\|v\|), \forall x \in \mathbb{R}^n, \forall v \in \mathbb{R}^d, \tag{6}$$

then, the system (1) is ISS with respect to the input v.

A function V that satisfies (5), (6) is called an ISS-Lyapunov function (LF) for the system (1).

Theorem 2
ISS of cascaded systems: (see [20]) Consider the following interconnected systems:

$$\begin{cases} x_2(k+1) = f_2(x_2(k), y_1(k), u(k)), \\ y_2 = h_2(x_2), \\ x_1(k+1) = f_1(x_1(k), v(k)), \\ y_1 = h_1(x_1) \end{cases} \tag{7}$$

Assume that the first system is IOS w.r.t the input v and output y_1 and the second system is IOS w.r.t the input (y_1,u) and the output y_2. Then, the interconnected system is IOS w.r.t the input (u,v) and output (y_1,y_2).

DOI: 10.1002/rnc

3. LINEAR PARAMETER VARYING SYSTEMS

We consider the following LPV system:

$$\Sigma_P : \begin{cases} x(k+1) = A(\theta(k))x(k) + Bu_c(k) + B_d d(k), \\ y(k) = Cx(k), \end{cases} \qquad x(0) = x_0 \tag{8}$$

where $x(k) \in \mathbb{R}^n$ is the state, $u(t) \in \mathbb{R}^m$ is the control input, $y(k) \in \mathbb{R}^p$ is the output, and $d(k) \in \mathbb{R}^d$ is the disturbance. The matrix $A \in \mathbb{R}^{n\times n}$ is a function of a time-varying parameter vector $\theta \in \mathbb{R}^{n_\theta}$. It is assumed that the parameter θ is bounded in a given compact set Θ i.e $\theta \in \Theta\ \forall k \in \mathbb{N}$. Matrix A can have different forms of dependence on the time-varying parameter θ. Among these forms, affine dependence and polytopic dependence are more appealing for synthesis and analysis purposes. Here, we consider the polytopic dependence. In the polytopic dependence form, A is written as:

$$A(\theta(k)) = \sum_{i=1}^{N} p_i(\theta(k))A_i, \tag{9}$$

where p_i is a continuous function $p_i : \Theta \to \mathbb{R}$ and A_i are matrices in $\mathbb{R}^{n\times n}$. Moreover, it is assumed that p_i belongs to the compact set:

$$\mathscr{P} = \{p = [p_1, \ldots, p_N] \in \mathbb{R}^N | p_i \geq 0, i = 1, \cdots, N, \sum_{i=1}^{N} p_i = 1\}. \tag{10}$$

Therefore, for all $\theta \in \Theta$, we have that $A(\theta(k))$ is in the convex hull of $A_1, \cdots, A_N$. In the rest of the paper for the sake of simplicity we omit the dependency of p_i on the $\theta(k)$ and use the notation $p_i(k)$ instead of $p_i(\theta(k))$ whenever it is necessary. We also mention that the affine dependency and polytopic dependency can be easily converted to each other.

Remark 1
In the above model, we assume that B and C are independent of the varying parameter θ. This is because we aim at obtaining conditions in terms of LMIs to design the gains of virtual actuator and sensor that are scheduled based on θ. It is possible to let the input and output matrices to be dependent on the varying parameter but design fixed gains for the virtual actuator and sensor. In both cases we can derive LMI conditions. In the following, we choose the first case where B and C are independent of θ. Obtaining the conditions for the second case is very similar.

3.1. Control Design

We assume that a nominal controller Σ_C is designed for the nominal system with the internal state $x_c \in \mathbb{R}^{n_c}$ and the reference input $r(t) \in \mathbb{R}^p$ which generates the control input u_c. It is assumed that the nominal closed loop system (Σ_P, Σ_C) is stable. We do not make any assumption about the structure of the controller. It could be for example a dynamic or static output feedback controller.

Assumption 1
IOS of the nominal closed loop system. The nominal closed loop system (Σ_P, Σ_C) is IOS w.r.t the inputs (r, d) and the output (u_c, x).

3.2. Faults

We consider both actuator and sensor faults. Actuator faults are modeled as events that change the input matrix of the LPV system from B to B_f. In the same way, sensor faults are modeled as events that change the measurement matrix from C to C_f. Therefore, the model of the faulty plant is given

DOI: 10.1002/rnc

by:

$$\Sigma_{P_f}: \begin{cases} x_f(k+1) = A(\theta(k))x_f(k) + B_f u_f(k) + B_d d(k), \\ y_f(k) = C_f x_f(k), \end{cases} \qquad (11)$$
$$x_f(0) = x_0.$$

3.3. Reconfiguration problem

In most of AFTC approaches, when a fault is detected and estimated a new controller Σ_{C_r} is designed and replaces Σ_C such that the stability of the closed-loop system that consists of $(\Sigma_{P_f}, \Sigma_{C_r})$ is guaranteed and it provides an acceptable performance. In this paper, we use the paradigm proposed in [6] in which instead of changing the nominal controller with a new controller designed for the faulty system, the nominal controller is kept in the loop and a reconfiguration block is inserted between the nominal controller and the faulty system, see Figure 1(c). The reconfiguration block receives as its input, the output of the nominal controller u_c and the output of the faulty system y_f and generates as its outputs, the input signal for the faulty system u_f and the input to the nominal controller y_c.

The LPV reconfiguration block is an LPV system with the internal state z:

$$\Sigma_R: \begin{cases} z(k+1) = A_r(\theta)(k)z(k) + B_r(\theta)u_c(k) + E_r(\theta)y_f(k), \\ y_c(k) = C_r(\theta)z(k) + F_r(\theta)y_f(k), \\ u_f(k) = G_r(\theta)z(k) + H_r(\theta)u_c(k), \end{cases} \qquad (12)$$
$$z(0) = z_0,$$

The reconfiguration block must be designed such that the overall closed-loop system $(\Sigma_{P_f}, \Sigma_R, \Sigma_C)$ is stable and some closed-loop performance requirements are satisfied. The series connection of the plant with the reconfiguration block (Σ_{P_f}, Σ_R) is called the reconfigured plant and the series connection of the nominal controller and the reconfiguration block (Σ_{P_f}, Σ_R) is called the reconfigured controller. Different goals in the design of the reconfiguration block may be considered and based on them different reconfiguration problems are defined. Here we consider the following problem.

Problem 1
Stability recovery for LPV systems. Consider the nominal LPV systems Σ_P (8) and the faulty LPV system Σ_{P_f} (11), find, if possible, a reconfiguration block Σ_R such that for all Σ_C that (Σ_C, Σ_P) is ISS w.r.t the input (r,d), we have $(\Sigma_{P_f}, \Sigma_R, \Sigma_C)$ is ISS w.r.t the input (r,d).

4. RECONFIGURATION BLOCK DESIGN

In this work, the reconfiguration block, Σ_R is realized by a virtual sensor, Σ_S and a virtual actuator Σ_A as depicted in Figure 2. The virtual sensor estimates the state of the faulty system $\hat{x}_f$ based on a model of the faulty plant and feedback of an injection of the output of the faulty system through gain L. The virtual actuator uses a reference model that is the same as the model of the nominal plant to generate a reference state $\tilde{x}$. The estimate of state of the faulty system $\hat{x}_f$ is compared with the reference state $\tilde{x}$. The difference between the estimate of the state of the faulty system and the state of the reference model, x_Δ, is then fed back through the gain M. The output injection gain L and the gain M are designed such that the estimation error goes to zero and at the same time the difference state (x_Δ) goes to zero. Consequently, states of the faulty system approach to the states of the reference model. In the following we describe the virtual actuator and sensor in details.

DOI: 10.1002/rnc

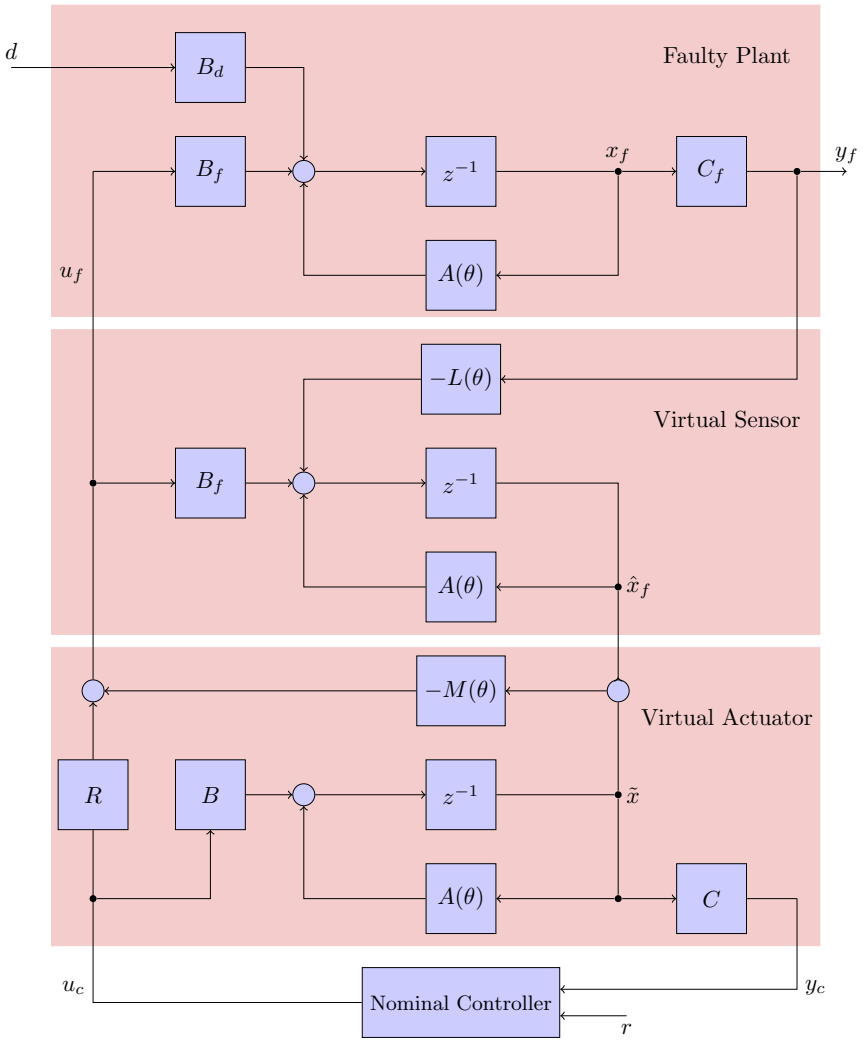

Figure 2. LPV virtual sensor and actuator in the closed loop system

The virtual actuator block has the following structure:

$$\Sigma_A : \begin{cases} \tilde{x}(k+1) = A(\theta)\tilde{x}(k) + Bu_c(k), \\ u_f(k) = -M(\theta)x_\Delta(k) - Ru_c(k), \\ y_c(t) = C\tilde{x}(k), \\ \tilde{x}(0) = \hat{x}_{f0}, \end{cases} \tag{13}$$

where $x_\Delta(k) = \tilde{x}(k) - \hat{x}_f(k)$ is the difference state, and M is a time-varying gain matrix that depends on θ which is defined as:

$$M(\theta(k)) = \sum_{i=1}^{N} p_i(k) M_i. \tag{14}$$

The virtual sensor is defined as:

$$\Sigma_S : \begin{cases} \hat{x}_f(k+1) = A_\delta(\theta)\hat{x}_f(k) + B_f u_f(k) - L(\theta)y_f(k), \\ u_f(k) = u_c(k), \\ \hat{x}_f(0) = \hat{x}_{f0}, \end{cases} \tag{15}$$

DOI: 10.1002/rnc

where $A_\delta(\theta) = A(\theta) + L(\theta)C_f$ and L is a time-varying gain matrix that depends on θ that is defined as:

$$L(\theta(k)) = \sum_{i=1}^{N} p_i(k) L_i. \tag{16}$$

To analyze the reconfigured plant we introduce the observation error defined as $e = \hat{x}_f - x_f$ and the difference state defined as $x_\Delta = \tilde{x} - \hat{x}_f$ and associated with them the observation error system Σ_e and the difference system Σ_Δ which are defined as follows. The observation error system is defined as:

$$\begin{aligned} \Sigma_e : e(k+1) &= A_\delta(\theta) e(k) + v(k), \\ e(0) &= \hat{x}_{f0} - x_0, \end{aligned} \tag{17}$$

where

$$v(k) = -B_d d(k), \tag{18}$$

and the difference system is defined as:

$$\begin{aligned} \Sigma_\Delta : x_\Delta(k+1) &= (A(\theta) + B_f M(\theta)) x_\Delta(k) + L(\theta) C_f e(k) + B_\Delta u_c(k), \\ x_\Delta(0) &= 0, \end{aligned} \tag{19}$$

where $B_\Delta = B + B_f R$. Dynamics of the system in terms of $\tilde{x}$ and the new introduced variables e and x_Δ are given by :

$$\begin{bmatrix} \tilde{x}(k+1) \\ e(k+1) \\ x_\Delta(k+1) \end{bmatrix} = \begin{bmatrix} A(\theta) & 0 & 0 \\ 0 & A(\theta) + L(\theta) C_f & 0 \\ 0 & L(\theta) C_f & A(\theta) + B_f M(\theta) \end{bmatrix} \begin{bmatrix} \tilde{x}(k) \\ e(k) \\ x_\Delta(k) \end{bmatrix} + \begin{bmatrix} B \\ 0 \\ B_\Delta \end{bmatrix} u_c(k) + \begin{bmatrix} 0 \\ -B_d \\ 0 \end{bmatrix} d(k), \tag{20}$$

$$y_c(k) = \begin{bmatrix} C & 0 & 0 \end{bmatrix} \begin{bmatrix} \tilde{x}(k) \\ e(k) \\ x_\Delta(k) \end{bmatrix}, \begin{bmatrix} \tilde{x}(0) \\ e(0) \\ x_\Delta(0) \end{bmatrix} = \begin{bmatrix} \hat{x}_{f0} \\ \hat{x}_{f0} - x_0 \\ 0 \end{bmatrix}. \tag{21}$$

We can see in (20) that the reference state $\tilde{x}$ is decoupled from the observation error e and the difference state. Also, the observation error is decoupled from the reference state, the difference state and the input u_c. The difference state is decoupled from the reference state. In the following we find sufficient conditions in terms of LMIs for the observation error and the difference system to be ISS and then we show that these conditions also guarantee the stability of the overall closed-loop system. In Theorem 3, we give the conditions for designing the virtual sensor gains L_i and in Theorem 4 we give the conditions for designing the virtual actuator gains M_i such that they are ISS respectively. Then, in Theorem 5, we show that separate design of these gains results in stability of the overall closed-loop system that consists of $\left(\Sigma_{P_f}, (\Sigma_S, \Sigma_A), \Sigma_C\right)$. In other words, separate design of the virtual actuator and virtual sensor gains yields stability of the overall closed-loop system.

4.1. Virtual Sensor Design

In the following we give LMI conditions for designing gains of virtual sensor and discuss how we can minimize its ISS gain and peak-to-peak gain.

Theorem 3
Consider the faulty LPV system (11). If there exist symmetric matrices $P_i = P_i^T$, matrices G_i and $U_i, i = 1, \cdots, N$ and a scalar $\sigma_d \geq 1$ such that the following set of LMIs are satisfied:

$$\begin{bmatrix} P_j - G_i - G_i^T & 0 & G_i A_i + U_i C_f & G_i \\ * & -I & I & 0 \\ * & * & -P_i & 0 \\ * & * & * & -\sigma_d I \end{bmatrix} < 0 \quad \forall i, j = 1, \cdots, N, \tag{22}$$

DOI: 10.1002/rnc

then, the virtual sensor Σ_S is an observer for the LPV system such that the observation error system (17) is GES for $d(k) = 0$. Moreover, the error dynamics (17) is ISS w.r.t the disturbance d with ISS gain $\gamma_d(s) = \|B_d\|\sigma_d s$. The observer gain is given by :

$$L(\theta) = \sum_{i=1}^{N} p_i(k) L_i,\ L_i = G_i^{-1} U_i. \tag{23}$$

Proof
See Appendix A.1. □

To minimize the ISS gain, the following optimization problem is solved.

$$\begin{aligned} &\min_{P_i, G_i, U_i, \sigma_d} \sigma_d \\ &s.t\ (22) \end{aligned} \tag{24}$$

The above optimization problem is a convex optimization problem with a set of LMI constraints which can be solved efficiently using available softwares such as YALMIP/SeDuMi or YALMIP/LMILAB [23].

Link to peak-to-peak gain:

The peak-to-peak gain of the observation error is defined as:

$$\sup_{0<\|d\|_\infty<\infty} \frac{\|e\|_\infty}{\|d\|_\infty}. \tag{25}$$

Corollary 1
If the LMIs (22) are satisfied then the error system (17) with the observer gain (23) admits a peak-to-peak gain smaller than $\|B_d\|\sigma_d$.

The proof is straightforward from (64) by taking the limit of κ to infinity and assuming $e(0) = 0$. Note that according to the corollary by minimizing the ISS gain we are also minimizing the upper bound on the peak-to-peak gain.

4.2. *Virtual Actuator Design*

In the following theorem we give conditions for the design of stabilizing gains for the virtual actuator such that the difference system is stable.

Theorem 4
Consider the faulty LPV system (11). If there exist symmetric matrices $Q_i = Q_i^T$ and matrices Y_i for $i = 1, \cdots, N$ and scalars $\sigma_a \geq 1$ and such that:

$$\begin{bmatrix} -Q_j & 0 & A_i Q_i + B_f Y_i & I \\ 0 & -I & Q_i & 0 \\ * & * & -Q_i & 0 \\ * & * & * & -\sigma_a I \end{bmatrix} < 0\ \forall i, j = 1, \cdots, N, \tag{26}$$

then, the difference system (19) associated with the virtual actuator is ISS with respect to the input (u_c, e). The virtual actuator gain is given by:

$$M(\theta(k)) = \sum_{i=1}^{N} p_i(k) M_i, \text{ with } M_i = Y_i Q_i^{-1}. \tag{27}$$

The ISS gain w.r.t. e is $\gamma_e(s) = \sigma_a c_1 \|C_f\| s$ where $c_1 = \max_{1 \leq i \leq N} \|L_i\|$ and the ISS gain w.r.t. u_c is $\sigma_a \|B_\Delta\|$. The ISS gain w.r.t. (u_c, e) is $\max(\sigma_a c_1 \|C_f\|, \sigma_a \|B_\Delta\|)$.

Prepared using rncauth.cls
DOI: 10.1002/rnc

Proof
See Appendix A.2. □

Note that the gain w.r.t. u_c is proportional to $\|B_\Delta\|$ and also the gain w.r.t. e is proportional to $c_1\|C_f\|$ which is sensible since the difference state is affected by e through the matrix $L(\theta)C_f$ and by the control signal u_c through the matrix B_Δ.

Minimization of the ISS gain of the virtual actuator can be formulated as the following optimization problem:

$$\min_{Q_i,Y_i,\sigma_a,} \sigma_a \quad s.t.\ (26) \tag{28}$$

The above optimization problem is a convex optimization problems with LMI constraints which can be solved efficiently using available softwares such as YALMIP/SeDuMi or YALMIP/LMILAB [23].

Link to peak-to-peak gain:
The peak-to-peak gain of the difference system is defined as:

$$\sup_{0<\|w\|_\infty<\infty} \frac{\|x_\Delta\|_\infty}{\|w\|_\infty}. \tag{29}$$

where $w = \begin{bmatrix} e & u_c \end{bmatrix}^T$.

Corollary 2
If the LMIs (26) are satisfied then the difference system (19) with the gains (27) admits a peak-to-peak gain smaller than $\max(\sigma_a c_1\|C_f\|, \sigma_a\|B_\Delta\|)$.

4.3. Combination of Virtual Sensor and Virtual Actuator

So far, we gave conditions for the design of the virtual actuator and the virtual sensor. The following lemma considers the stability of the cascade connection of the error system and the difference system and states that their interconnection is ISS if they are designed based on the above theorems. The interconnection is given by:

$$\begin{bmatrix} e(k+1) \\ x_\Delta(k+1) \end{bmatrix} = \begin{bmatrix} (A(\theta)+L(\theta)C_f) & 0 \\ L(\theta)C_f & (A(\theta)+B_f M(\theta)) \end{bmatrix} \begin{bmatrix} e(k) \\ x_\Delta(k) \end{bmatrix} + \begin{bmatrix} 0 \\ B_\Delta \end{bmatrix} u_c(k) + \begin{bmatrix} -B_d \\ 0 \end{bmatrix} d(k) \tag{30}$$

.

Lemma 1
If observer gains of the error system (17) and gains of the difference system (19) are designed based on the conditions in Theorem 3 and 4, then the interconnection (Σ_S, Σ_A) given by (30) is also ISS. The ISS gain of the interconnection w.r.t. d is $c_2\sqrt{\mu\sigma_d c_4}s$ and w.r.t u_c is $c_3\sqrt{\sigma_a c_4}s$ where

$$c_2 = \|B_d\|,\ c_3 = \|B_\Delta\|, \mu = \sigma_a c_1^2\|C_f\|^2 + 1,\ c_4 = \max(\mu\sigma_d, \sigma_a). \tag{31}$$

Proof
See Appendix A.3. □

DOI: 10.1002/rnc

4.4. *Stability of the Closed-loop System*

The following theorem states that if we design the virtual actuator and the virtual sensor independently based on the previous theorems, then we can guarantee that the closed-loop reconfigured system that consists of the interconnection $\left(\Sigma_{P_f},(\Sigma_S,\Sigma_A),\Sigma_C\right)$ is ISS w.r.t to the input (r,d).

Theorem 5
Consider the faulty LPV system (11). Assume that Assumption 1 holds. If there exist $M_i(\theta),L_i(\theta)$ such that conditions (22) and (26) are satisfied, then the closed-loop reconfigured system $(\Sigma_{P_f},\Sigma_S,\Sigma_A,\Sigma_C)$ with $M_i=Y_iQ_i^{-1}$ and $L_i=G_i^{-1}U_i, i=1,\cdots,N$ is ISS w.r.t the input (r,d).

Proof
See Appendix A.4.

□

4.5. *Control Reconfiguration Algorithm*

The overall algorithm for the proposed fault-tolerant control method is summarized in Algorithm 1. We assume that there is a fault detection and isolation (FDI) module which detects and isolates the fault. When a fault is isolated, the system is reconfigured based on the type of the fault. Estimation of the parameters of the faulty system can be performed using available results on identification of LPV systems, for example see [24] or [25] and references therein. The proposed method in this paper, works as long as there is no missed detection and no false positive alarm and the estimation error is small such that the system is robust to the uncertainties in the estimated parameters.

Three different cases are possible: sensor fault but no actuator fault, actuator fault but no sensor fault, simultaneous sensor and actuator fault. If there is only sensor faults and no actuator faults, we only need to reconfigure the loop by locating the virtual sensor in the loop. In this case the virtual sensor is acting as an observer which estimates the states of the system form the healthy measurements. In this case, the parameters of the faulty system C_f is received from the FDI module and the gains of the virtual sensor are obtained by solving the optimization problem (24). The estimated state of the faulty system is multiplied by the output matrix of the nominal system, C and then injected as input to the nominal controller i.e. $y_c=C\hat{x}_f$. Since the input matrix B and the internal dynamics $A(\theta)$ are not changed the dynamics viewed by the nominal controller is the same of that of the reference model (the nominal plant).

When there is only actuator faults, the virtual sensor gains are the same as the gains for the nominal plant since the C and A matrix are not changed. In this case, the virtual sensor acts as an observer that estimates the state of the faulty system. Then, the gains of the virtual actuator,M_i's , are designed by solving the optimization problem (28). The the reference model is initialized with the estimate of the state of the faulty system obtained by virtual sensor i.e $\tilde{x}(k_r)=\hat{x}_f(k_r)$, where k_r is the time of reconfiguration. In order to avoid large over-shoots, it is possible to wait for some sample time so that the virtual sensor converges such that the estimation error, $\hat{x}_f-x_f$, becomes small and then initialize the reference model and reconfigure the system.

In case both actuator and sensor faults have occurred, the gains of the virtual sensor L_i must also be updated since the output matrix in changed to C_f in this case. C_f is received from the FDI module, the gains of the virtual sensor L_i are updated by solving (24), the gains of the virtual actuator, M_i's, are obtained by solving (28) and the reference model is initialized by the estimate of the state of the system. Finally, the loop is reconfigured by locating both virtual sensor and actuator in the loop, i.e. the reconfigured loop is $(\Sigma_{P_f},\Sigma_S,\Sigma_A,\Sigma_C)$.

In designing the virtual actuator we choose R to minimize $\|B\|_\Delta$(see line 16 of Algorithm 1). This is because the ISS gain of the virtual actuator w.r.t. (u_c,e) is given by $\max(\sigma_a c_1\|C_f\|,\sigma_a\|B_\Delta\|)$. Note that c_1 is determined by the maximum of the norms of the virtual sensor gains that are obtained separately here. The only variable that we can manipulate here through choosing R is $\|B_\Delta\|$.

DOI: 10.1002/rnc

Algorithm 1 Fault-Tolerant Control design for LPV system using virtual actuator and sensor

Given The parameters of the nominal LPV system Σ_P: $A_i, i = 1, \cdots, N$, B, B_d, C.
$C_f \leftarrow C$
Solve the optimization problem (24) ▷ To design a stabilizing virtual sensor
$L_i \leftarrow G_i^{-1} U_i, i = 1, \cdots, N$ ▷ Gains of the virtual sensor
repeat
    Run the nominal loop that consists of (Σ_P, Σ_C)
until an actuator or sensor fault is isolated.
if there is a sensor fault **then**
    Update C_f from the FDI module.
    Solve the optimization problem (24) ▷ Re-design the virtual sensor
    $L_i \leftarrow G_i^{-1} U_i, i = 1, \cdots, N$. ▷ Update the gains of the virtual sensor
end if
if there is an actuator fault **then**
    Update B_f from the FDI module.
    Update the virtual sensor with B_f.
    Choose R to minimize $\|B_\Delta\|$
    Solve the optimization problem (28) ▷ Design the virtual actuator
    $M_i \leftarrow Y_i Q_i^{-1}, i = 1, \cdots, N$. ▷ The gains of the virtual actuator
end if
if there is only sensor fault but no actuator fault **then**
    $y_c \leftarrow C\hat{x}_f$ ▷ Put the virtual sensor in the loop.
    Run the reconfigured loop consisting of $(\Sigma_{P_f}, \Sigma_S, \Sigma_C)$
else
    $\tilde{x}(k_r) \leftarrow \hat{x}_f(k_r)$ ▷ Initialization of the reference model at the time of reconfiguration
    Run the reconfigured loop consisting of $(\Sigma_{P_f}, \Sigma_S, \Sigma_A, \Sigma_C)$
end if

4.6. Special Cases: Static Reconfiguration Blocks

A special case of the above solutions is when the virtual actuator and virtual sensor can be realized using a static block [7]. Consider the case of an actuator fault. In this situation, if the image of the nominal input matrix B is a subset of the image of the faulty input matrix B_f, then all control signals generated by the healthy actuator can be generated by the faulty actuator. Therefore, the system can be reconfigured by inserting a static block S before u_f i.e $u_f = S_B u_c$. The general solution is given by the matrix S such that:

$$B_f S_B = B. \tag{32}$$

The solution to this problem exists if:

$$\text{im } B \subseteq \text{im } B_f, \tag{33}$$

where im $B = \{Bu : u\mathbb{R}^m\}$. An equivalent condition is:

$$\text{rank}(B_f) = \text{rank}(\begin{bmatrix} B_f & B \end{bmatrix}) \tag{34}$$

A similar approach can be used for the case of sensor fault. In this case the faulty measurement is corrected through a static gain S_C, therefore $y_c = S_C y_f$. Therefore, matrix S_C must satisfy:

$$S_C C_f = C. \tag{35}$$

The above condition is satisfied if and only if:

$$\text{rank}(C_f) = \text{rank}(\begin{bmatrix} C_f \\ C \end{bmatrix}). \tag{36}$$

DOI: 10.1002/rnc

5. EXAMPLE

We consider the following LPV system:

$$x(k+1) = \sum_{i=1}^{N} p_i(k)A_i + Bu(k) + B_d(k)$$
$$y(k) = Cx(k) \tag{37}$$

with the following parameters:

$$A_1 = \begin{bmatrix} 0.7786 & 0.9908 & 0.1270 \\ 0.1616 & 0.8443 & 0.8144 \\ 0.9214 & 0.9747 & 0.7825 \end{bmatrix}, \quad A_2 = \begin{bmatrix} 0.3984 & 0.3263 & 0.7764 \\ 0.7806 & 0.9886 & 0.1297 \\ 0.8814 & 0.4718 & 0.3110 \end{bmatrix},$$
$$A_3 = \begin{bmatrix} 0.3049 & 0.4247 & 0.8979 \\ 0.8448 & 0.2485 & 0.6921 \\ 0.7558 & 0.9160 & 0.3636 \end{bmatrix}, \quad A_4 = \begin{bmatrix} 0.1194 & 0.3964 & 0.2454 \\ 0.1034 & 0.2515 & 0.4983 \\ 0.6981 & 0.8655 & 0.2403 \end{bmatrix},$$
$$B = \begin{bmatrix} 0.984 & 0.7409 \\ 0.9237 & 0.9118 \\ 0 & 0 \end{bmatrix}, \quad B_d = \begin{bmatrix} 0.02 \\ 0.02 \\ 0.02 \end{bmatrix},$$
$$C = \begin{bmatrix} 0.3815 & 0.6916 & 0.7183 \end{bmatrix}, \tag{38}$$

We mention that all the matrices $A_1, \cdots, A_4$ are unstable and therefore the open-loop system is unstable. To test the method we consider the extreme change of the parameters p_i so that they take values randomly between 0 and 1 subject to the constraint that their sum is equal to 1. The details of the nominal controller is not important for our approach but for the sake of completeness we also give the details here. A gain-scheduled H_∞ static-output feedback (SOF) controller of the form $u = \sum_{i=1}^{N} p_i(k)K_i y(k)$ is designed for the nominal system using the method in Appendix A.5. The corresponding gains are:

$$K_1 = \begin{bmatrix} 3.2224 \\ -4.9456 \end{bmatrix}, \; K_2 = \begin{bmatrix} -0.7580 \\ -0.4070 \end{bmatrix}, \; K_3 = \begin{bmatrix} 0.5869 \\ -1.9773 \end{bmatrix}, \; K_4 = \begin{bmatrix} 0.9532 \\ -1.7546 \end{bmatrix}. \tag{39}$$

The H_∞ gain of the designed controller is 0.4016. A simulation of the nominal system and nominal controller is given in Figure 3

5.1. *Partial loss of the actuator gain*

In the first scenario we consider partial loss of the actuator gain. As a result of this fault the input matrices are changed to:

$$B_f = 0.4B. \tag{40}$$

The nominal controller with the faulty system with 60% loss of actuator gain is unstable. This is depicted in Figure 4 where the fault occurs at $k = 30$. In this case the reconfiguration block is realized by a virtual sensor and a virtual actuator. The virtual sensor is basically an observer for the faulty system that estimates the state of the faulty system. Since the C matrix is not changed, the gains of the virtual sensor would be the same as the gains of an observer designed for the nominal system. We use (24) with nominal output matrix C and obtain the virtual sensor gains. The gains are given as:

$$L_1 = \begin{bmatrix} -0.8989 \\ -1.039 \\ -1.42 \end{bmatrix}, \; L_2 = \begin{bmatrix} -0.8179 \\ -0.9723 \\ -0.8031 \end{bmatrix}, \; L_3 = \begin{bmatrix} -0.899 \\ -1.014 \\ -1.163 \end{bmatrix}, \; L_4 = \begin{bmatrix} -0.4452 \\ -0.4938 \\ -0.9263 \end{bmatrix}, \tag{41}$$

σ_d of the virtual sensor is obtained as 6.3116 and therefore its ISS gain is 0.2184.

DOI: 10.1002/rnc

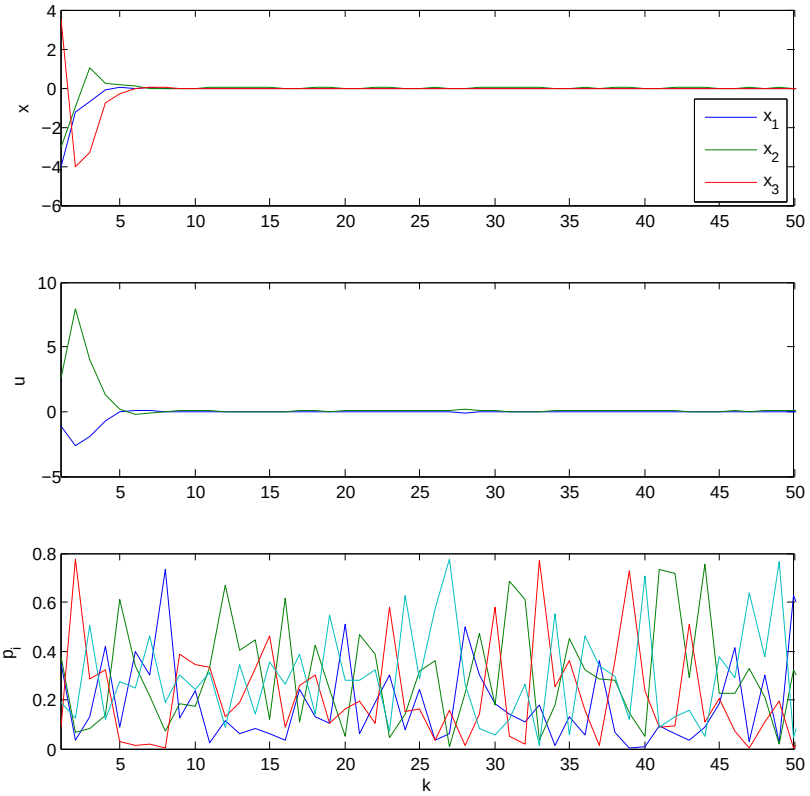

Figure 3. Simulation of the nominal closed-loop

To design the virtual actuator, the gain R is designed such that it gives us the possibility to minimize σ_a. Since u_c is amplified by B_Δ and $B_\Delta = B + B_f R$, we choose R as:

$$R = -B_f^T (B_f B_f^T)^{-1} B.$$

Consequently, $B_\Delta = 0$. The virtual actuator gains are obtained by solving the optimization problem (28). The gains are:

$$M_1 = \begin{bmatrix} -8.039 & -4.549 & 4.507 \\ 6.93 & 1.48 & -7.452 \end{bmatrix}, M_2 = \begin{bmatrix} 1.714 & 4.589 & -7.291 \\ -4.664 & -7.781 & 6.753 \end{bmatrix},$$
$$M_3 = \begin{bmatrix} 3.287 & -3.189 & -3.854 \\ -6.32 & 1.732 & 1.682 \end{bmatrix}, M_4 = \begin{bmatrix} -1.351 & -3.027 & 1.429 \\ 0.5039 & 1.629 & -3.027 \end{bmatrix}, \quad (42)$$

We assume that the fault is detected and isolated after 15 sample times. The reference system is initialized with the estimate of the states from the virtual sensor and then the virtual actuator is activated. Figure 5 shows the simulation result. The observation error shows that the virtual sensor estimates effectively the state of the nominal as well as the faulty system. As we can see both the observation error e and the difference system x_Δ are stable and the system is stabilized by the virtual actuator. The σ_a of the virtual actuator is obtained as 6.1954. Therefore, its ISS gain w.r.t. (u_c, e) is obtained as 13.07.

DOI: 10.1002/rnc

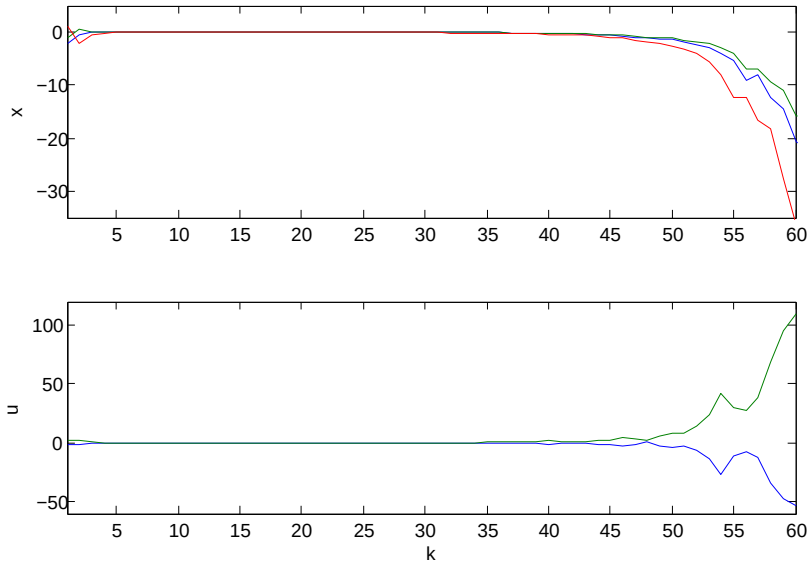

Figure 4. Simulation of the nominal controller with faulty system with 60% loss of actuator gain. The fault occurs at $k = 30$.

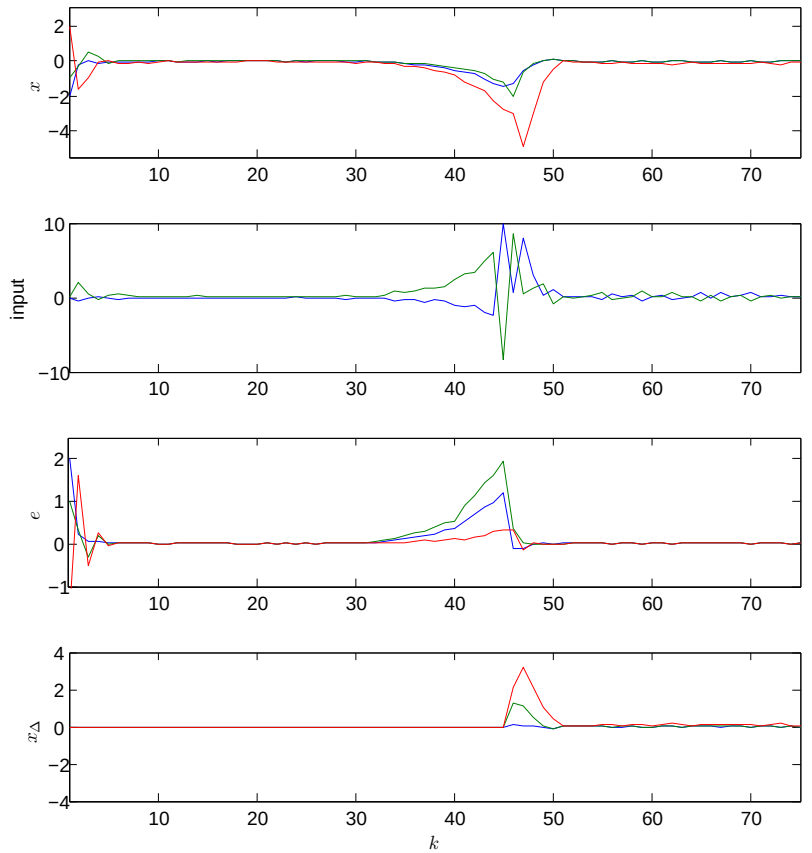

Figure 5. Simulation of the faulty system with 60% loss of actuator gain with reconfiguration block. The fault occurs at $k = 30$, and the virtual actuator is activated at $k = 45$.

DOI: 10.1002/rnc

5.2. *Complete loss of second actuator*

In this scenario we consider total loss of the second actuator. Consequently, the input matrix changes to:

$$B_f = \begin{bmatrix} 0.984 & 0 \\ 0.9237 & 0 \\ 0 & 0 \end{bmatrix}.$$

As a result of this fault the loop consisting of the nominal controller and the faulty system becomes unstable. As before, the reconfiguration block is realized by a virtual sensor and a virtual actuator. The gain of the virtual sensor are the same as before since the C matrix is the same. The matrix R is chosen such that we are minimizing the Frobenius norm of B_Δ. The matrix R is given by:

$$R = \begin{bmatrix} 1 & R_{12} \\ 0 & 0 \end{bmatrix}$$

where R_{12} is obtained by minimizing the Frobenius norm of the second column of $B + B_f R$ as $R_{12} = 0.8702$. The gains of the virtual actuator are obtained by solving (28) as:

$$\begin{aligned} M_1 &= \begin{bmatrix} -0.9289 & -1.419 & -0.8561 \\ 0 & 0 & 0 \end{bmatrix}, M_2 = \begin{bmatrix} -0.9644 & -0.9026 & -0.5506 \\ 0 & 0 & 0 \end{bmatrix}, \\ M_3 &= \begin{bmatrix} -0.8802 & -0.6972 & -0.9688 \\ 0 & 0 & 0 \end{bmatrix}, M_4 = \begin{bmatrix} -0.3217 & -0.5921 & -0.462 \\ 0 & 0 & 0 \end{bmatrix}. \end{aligned} \tag{43}$$

Since the second row of M_i's are replaced by zero the input to the lost actuator is replaced by zero. As it is expected in this case the ISS gain of the virtual actuator increases and we get $\sigma_a = 10.3970$ and $\gamma_a = 21.93s$. The simulation results are depicted in Figure 6. The fault occurs at $k = 30$. We assume that the fault is detected and isolated after 5 samples. As it can be seen, the reconfiguration block effectively stabilizes the faulty system. Note that in Figure 6, x_Δ before occurrence of fault is zero because the virtual actuator is not active in that period. Also, notice that the input to the second actuator is zero after the reconfiguration time $k = 35$.

5.3. *Simultaneous sensor and actuator fault*

In this scenario, we consider simultaneous sensor and actuator fault. The second actuator is totally lost and the C matrix is changed to:

$$C_f = \begin{bmatrix} 0.7638 & 1.3832 & 0 \end{bmatrix}.$$

The reconfiguration block is realized by a virtual sensor and a virtual actuator. The gains of the virtual sensor are obtained as:

$$L_1 = \begin{bmatrix} -0.8836 \\ -0.8482 \\ -1.248 \end{bmatrix}, L_2 = \begin{bmatrix} -0.6994 \\ -0.8848 \\ -0.7754 \end{bmatrix}, L_3 = \begin{bmatrix} -0.7583 \\ -0.8319 \\ -0.9484 \end{bmatrix}, L_4 = \begin{bmatrix} -0.3547 \\ -0.3975 \\ -0.8405 \end{bmatrix}, \tag{44}$$

and the matrix R is chosen as in 5.2. The gain of the virtual actuator are given by solving (28):

$$\begin{aligned} M_1 &= \begin{bmatrix} -0.9257 & -1.418 & -0.8585 \\ 0 & 0 & 0 \end{bmatrix}, M_2 = \begin{bmatrix} -0.9671 & -0.9002 & -0.5575 \\ 0 & 0 & 0 \end{bmatrix}, \\ M_3 &= \begin{bmatrix} -0.8802 & -0.691 & -0.9658 \\ 0 & 0 & 0 \end{bmatrix}, M_4 = \begin{bmatrix} -0.3237 & -0.5946 & -0.4625 \\ 0 & 0 & 0 \end{bmatrix}, \end{aligned} \tag{45}$$

The simulation results are given in Figure 7. As it is expected in this case σ_d increases to 7.85 and γ_a increases to $27.07s$. The fault occurs at $k = 30$. We assume that the fault is detected and isolated after 5 seconds. As it can be seen, the reconfiguration block effectively stabilizes the system.

DOI: 10.1002/rnc

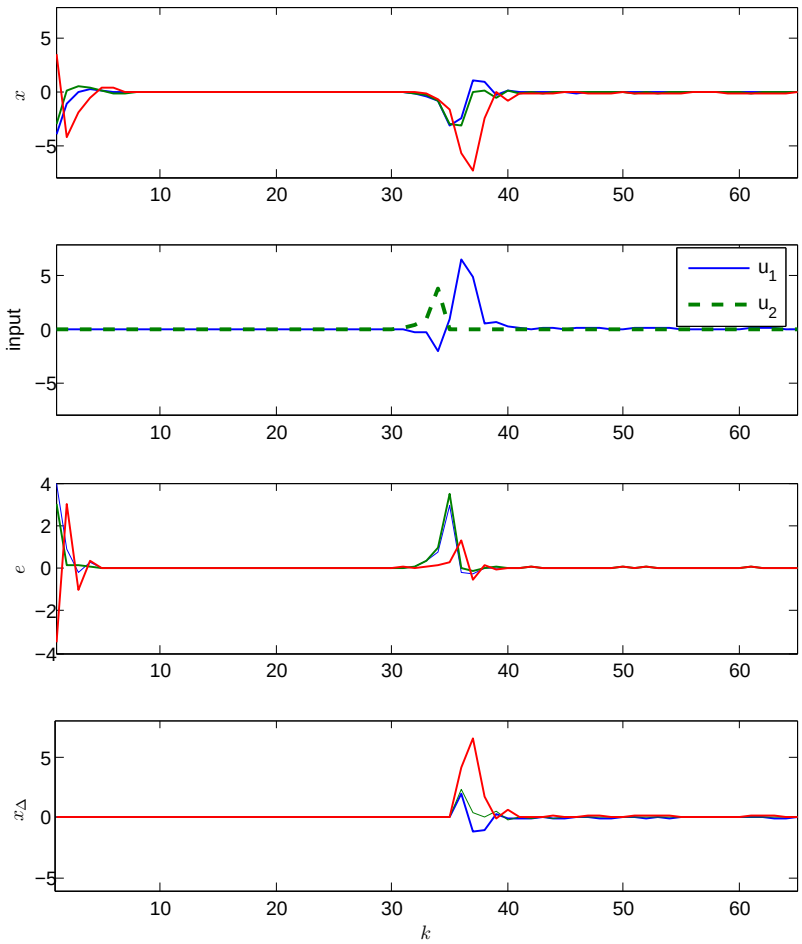

Figure 6. Simulation of the faulty system with total loss of the second actuator with reconfiguration block. The fault occurs at $k = 30$, and the virtual actuator is activated at $k = 35$.

5.4. FTC control of an induction motor

We consider the problem of stator current control for an induction motor. A squirrel cage induction motor is considered here. Using the dynamic (d,q) frame, the nonlinear model of the induction motor is given as [26]:

$$\begin{cases} \dot{\phi}_a = a_1\phi_a - n_p\omega\phi_b + a_2 i_a, \\ \dot{\phi}_b = n_p\omega\phi_a + a_2 i_b, \\ \dot{i}_a = a_3\phi_a + a_4\omega\phi_b - \gamma i_a + a_5 u_1, \\ \dot{i}_b = -a_4\omega\phi_a + a_3\phi_b - \gamma i_b + a_5 u_2, \\ y = \begin{bmatrix} i_a & i_b \end{bmatrix}^T, \end{cases} \tag{46}$$

where ω is the rotor speed, ϕ_a, ϕ_b are the (d,q) projection of the rotor flux, i_a, i_b are the (d,q) projection of the stator currents, and u_1, u_2 are the stator voltages. The parameters are defined as follows: $a_1 = -1/T_r, a_2 = L_{sr}/T_r, a_3 = L_{sr}/(T_r\sigma L_s L_r), a_4 = n_p L_{sr}/(\sigma L_s L_r)$ and $a_5 = 1/(\sigma L s)$ where $T_r = L_r/R_r, \gamma = \frac{R_s}{L_s\sigma} + \frac{L_{sr}^2}{L_s\sigma L_r T_r}$, and $\sigma = 1 - \frac{L_{sr}^2}{L_s L_r}$. The values of the parameters are given in Table I and are taken from [26].

In this example, we focus on the problem of controlling the current of the system where the current must follow a given reference. If we consider the rotor speed as a parameter, then the nonlinear

DOI: 10.1002/rnc

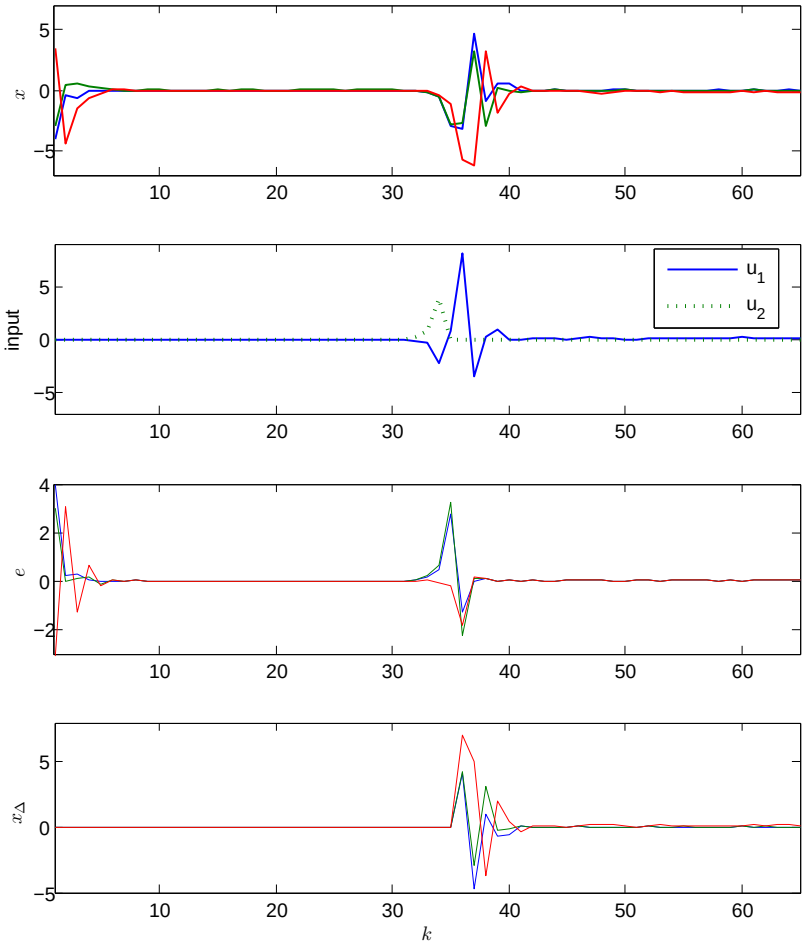

Figure 7. Simulation of the faulty system with total loss of the second actuator and sensor fault. The fault occurs at $k = 30$, and the reconfiguration block is activated at $k = 35$.

Table I. parameter values of the induction motor

Description	Parameters	Value	Units
Stator inductance	L_s	0.47	H
Rotor inductance	L_r	0.47	H
Mutual inductance	L_{sr}	0.44	H
Leakage factor	σ	0.12	
Stator Resistance	R_s	0.8	Ω
Rotor Resistance	R_r	3.6	Ω
Number of pole pairs	n_p	2	

system can be modeled as an LPV system as follows:

$$\begin{cases} \dot{x} = (A_0 + \omega A_1)x + Bu, \\ y = Cx, \end{cases} \tag{47}$$

DOI: 10.1002/rnc

where

$$A_0 = \begin{bmatrix} a_1 & 0 & a_2 & 0 \\ 0 & a_1 & 0 & a_2 \\ a_3 & 0 & -\gamma & 0 \\ 0 & a_3 & 0 & -\gamma \end{bmatrix}, A_1 = \begin{bmatrix} 0 & -n_p & 0 & 0 \\ n_p & 0 & 0 & 0 \\ 0 & a_4 & 0 & 0 \\ -a4 & 0 & 0 & 0 \end{bmatrix}, \tag{48}$$

$$B = \begin{bmatrix} 0 & 0 \\ 0 & 0 \\ a_5 & 0 \\ 0 & a_5 \end{bmatrix}, C = \begin{bmatrix} 0 & 0 & 1 & 0 \\ 0 & 0 & 0 & 1 \end{bmatrix}. \tag{49}$$

where $\omega \in [-110, 110]$. The system is discretized with a sample time of $T_s = 2$ms and an LPV model of it is obtained with introducing $p_1 = \frac{\omega - \underline{\omega}}{\overline{\omega} - \underline{\omega}}$, $p_2 = 1 - p_1$ where $\underline{\omega} = -110$ and $\overline{\omega} = 110$. An LPV static output feedback controller is designed to track the reference signal $\left[i_{a_r}, i_{b_r}\right]^T$ system using the method given in Appendix A.5. The gains are as follows:

$$K_1 = \begin{bmatrix} 7.7277 & -0.5076 \\ 0.5076 & 7.7277 \end{bmatrix}, K_2 = \begin{bmatrix} 7.7277 & 0.5076 \\ -0.5076 & 7.7277 \end{bmatrix} \tag{50}$$

Simulation of the response of the controlled system for $\omega = 88$ is given in Figure 8 and simulation results for 10 equally spaced value of ω is given in Figure 9 . We consider loss of measurement of i_b

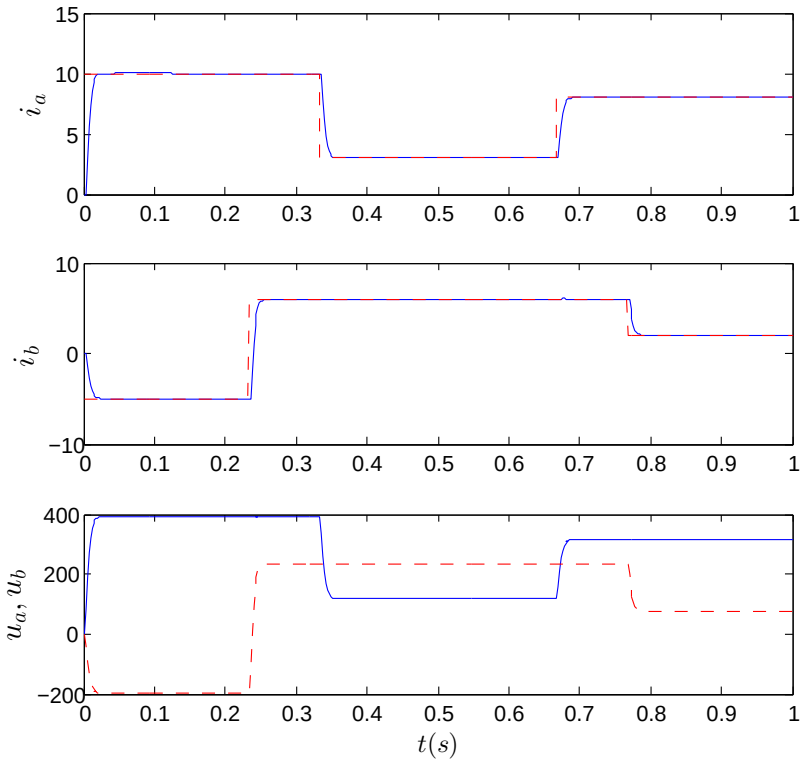

Figure 8. Simulation of the induction motor with SOF controller and $\omega = 88$ rad/s. Top: i_a, solid and i_{a_r} dashed, Middle: i_b, solid and i_{b_r} dashed, Bottom: u_a solid, u_b dashed.

as well as 40% loss of actuator gains. Simulation of the faulty system with 10 equally spaced values of ω in the range -110 to 110 is given in Figure 10. In the simulation, we assume that the inputs u_a and u_b saturate at ± 1000. As we see from the simulation, i_b cannot track the given reference any more and also the tracking performance of i_a is deteriorated significantly.

DOI: 10.1002/rnc

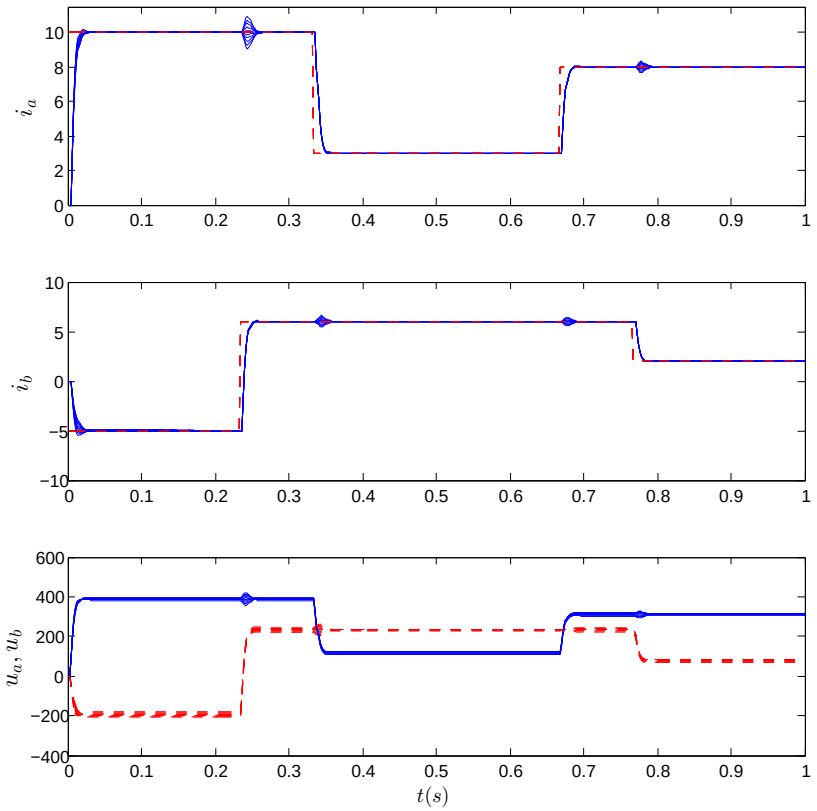

Figure 9. Simulation of the induction motor with SOF controller and 10 equally spaced values of ω in the range -110 to 110 . Top: i_a, solid and i_{a_r} dashed, Middle: i_b, solid and i_{b_r} dashed, Bottom: u_a solid, u_b dashed.

We use the method proposed in this paper and design a virtual actuator and a virtual sensor to reconfigure the system. The simulation results are given in Figure 11 which shows the simulation results for 10 equally spaced values of ω in the range $[-110, 110]$. As it is demonstrated, using a virtual sensor and a virtual actuator, we can regain tracking of i_b. Moreover, the tracking performance of i_a is better than the case where reconfiguration is not used. The bottom of the figure shows u_a and u_b which are the outputs of the virtual actuator i.e. the input to the faulty system. Note that the control efforts are increased compared to the case of fault-free system.

Comparison with AFTC using Controller Re-design: To compare our results with cases where we have the possibility of redesigning the controller, we use the following AFTC method. An observer is designed for the faulty system to estimate the missing measurement and then the SOF is re-designed based on the model of the faulty system using the method in Appendix A.5 with $B = B_f$. The nominal controller is then replaced with the re-designed controller. The simulation results are depicted in Figure 12. The results show that our proposed reconfiguration method and the re-designed AFTC method have similar performances with similar control efforts.

6. CONCLUSION

In this paper we presented a new method for fault tolerant control of linear parameter varying systems (LPV) using a reconfiguration block. We considered discrete time LPV systems with both sensor and actuator faults. The main idea of the method is to insert a reconfiguration block between the plant and the nominal controller such that the fault tolerant goal is achieved without re-designing the nominal controller. We do not need any knowledge about the nominal controller

DOI: 10.1002/rnc

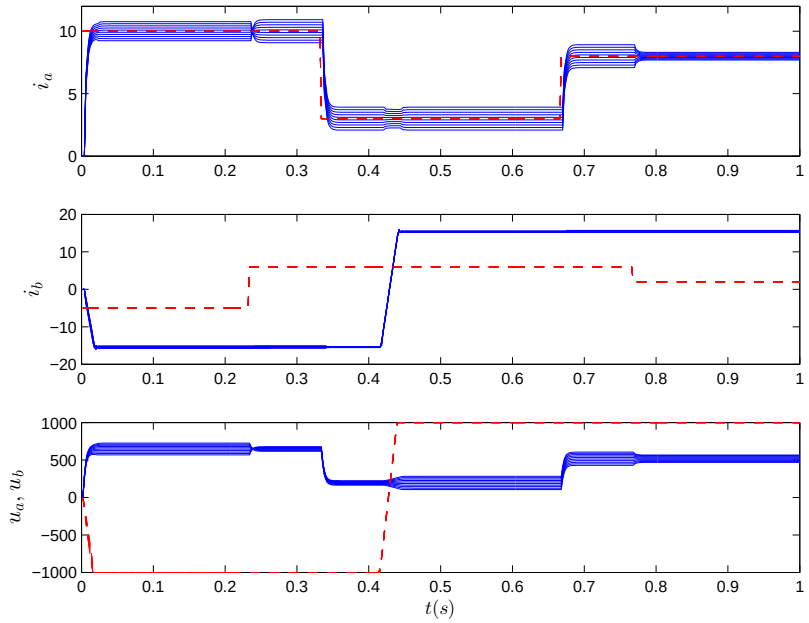

Figure 10. Simulation of the induction motor with SOF controller and 10 equally spaced values of ω in the range -110 to 110 subject to loss of measurement of i_b and 40% loss of actuator gains. Top: i_a, solid and i_{a_r} dashed, Middle: i_b, solid and i_{b_r} dashed, Bottom: u_a solid, u_b dashed.

and it is only assumed that the loop consisting of the nominal controller and the nominal system is stable. The reconfiguration block is realized by a virtual actuator and a virtual sensor. We show that by separately designing input-to-state stable (ISS) virtual sensor and actuators, the input-to-state stability of the closed loop reconfigured system is guaranteed. We derive sufficient conditions in terms of LMIs for ISS of the virtual sensor and actuator. Performance of the reconfiguration block in terms of ISS gains is derived and is optimized by convex optimization. The efficiency of the method is demonstrated by means of a numerical example as well as an example of stator current control of an induction motor.

REFERENCES

1. Blanke M, Izadi-Zamanabadi R, Bogh SA, Lunau CP. Fault-tolerant control systems-a holistic view. *Control Engineering Practice* 1997; **5**(5):693–702.
2. Patton RJ. Fault-tolerant control systems: The 1997 situation. *3rd IFAC symposium on fault detection supervision and safety for technical processes*, vol. 3, 1997; 1033–1054.
3. Jiang J. Fault-tolerant control systems-an introductory overview. *Acta Automatica Sinica* 2005; **31**(1):161–174.
4. Isermann R. *Fault-diagnosis systems*. Springer Verlag, 2006.
5. Blanke M, Kinnaert M, Lunze J, Staroswiecki M. *Diagnosis and Fault-Tolerant Control*. Springer-Verlag, 2006.
6. Niemann H, Stoustrup J. Controller reconfiguration based on LTR design. *Proceedings of 42nd IEEE Conference on Decision and Control*, vol. 3, 2003; 2453 – 2458 Vol.3, doi:10.1109/CDC.2003.1272988.
7. Steffen T. *Control reconfiguration of dynamical systems: linear approaches and structural tests*. Springer, 2005.
8. Lunze J, Steffen T. Control reconfiguration after actuator failures using disturbance decoupling methods. *Automatic Control, IEEE Transactions on* 2006; **51**(10):1590–1601.
9. Seron MM, De Don JA, Richter J. Fault tolerant control using virtual actuators and set-separation detection principles. *International Journal of Robust and Nonlinear Control* 2012; **22**(7):709–742, doi:10.1002/rnc.1719. URL http://dx.doi.org/10.1002/rnc.1719.
10. Richter JH, Heemels W, van de Wouw N, Lunze J. Reconfigurable control of PWA systems with actuator and sensor faults: stability. *47th IEEE Conference on Decision and Control*, 2008; 1060–1065.
11. Richter J, Lunze J. Reconfigurable control of hammerstein systems after actuator faults. *Proceedings of the 17th IFAC Word Congress*, 2008; 3210–3215.
12. Richter J, Heemels W, van de Wouw N, Lunze J. Reconfigurable control of piecewise affine systems with actuator and sensor faults: stability and tracking. *Automatica* 2011; **47**(4):678–691.
13. Richter JH. *Reconfigurable Control of Nonlinear Dynamical Systems*. Springer, 2011.

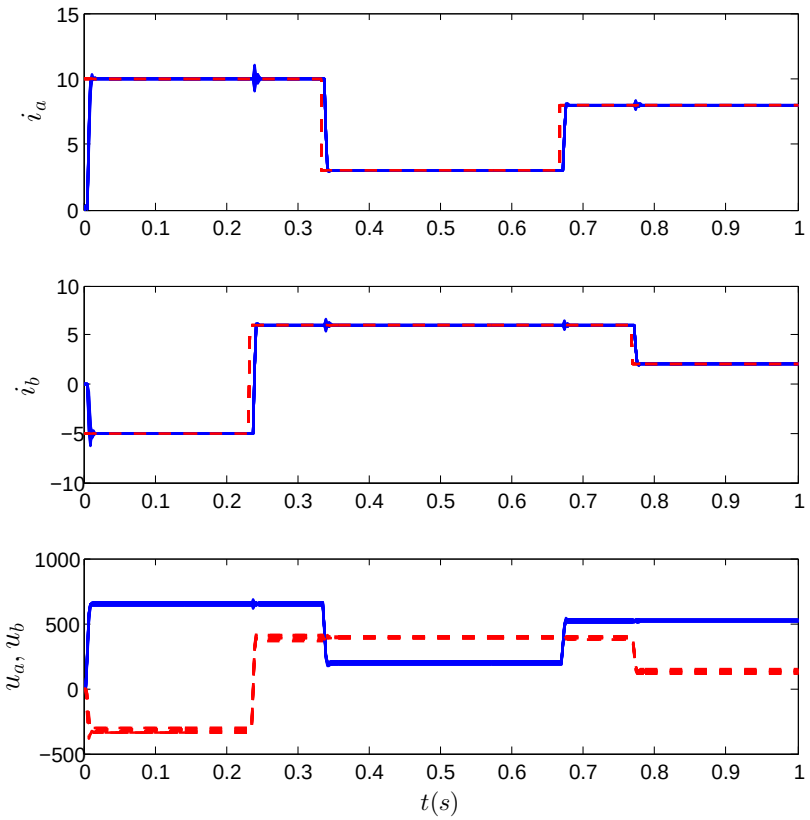

Figure 11. Simulation of the reconfigured system with 10 equally spaced values of ω in the range -110 to 110 subject to loss of measurement of i_b and 40% loss of actuator gains. Top: i_a, solid and i_{a_r} dashed, Middle: i_b, solid and i_{b_r} dashed, Bottom: Output of the virtual actuator u_a solid, u_b dashed.

14. Richter J, Seron M, De Dona JA. Virtual actuator for Lure systems with lipschitz-continuous nonlinearity. *8th IFAC Symposium on Fault Detection, Supervision, and Safety for Technical Processes*, vol. 8, Mexico City, Mexico, 2012; 222–227.
15. Khosrowjerdi MJ, Barzegary S. Fault tolerant control using virtual actuator for continuous-time lipschitz nonlinear systems. *International Journal of Robust and Nonlinear Control* 2013; doi:http://dx.doi.org/10.1002/rnc.3002.
16. de Oca S, Puig V. Fault-tolerant control design using a virtual sensor for LPV systems. *2010 Conference on Control and Fault-Tolerant Systems (SysTol),*, 2010; 88–93.
17. Nazari R, Seron M, Don JD. Fault-tolerant control of systems with convex polytopic linear parameter varying model uncertainty using virtual-sensor-based controller reconfiguration. *Annual Reviews in Control* 2013; **37**(1):146 – 153, doi:http://dx.doi.org/10.1016/j.arcontrol.2013.04.004. URL http://www.sciencedirect.com/science/article/pii/S1367578813000138.
18. Tabatabaeipour SM, Stoustrup J, Bak T. Control reconfiguration of LPV systems using virtual sensor virtual actuator. *8th IFAC Symposium on Fault Detection, Supervision, and Safety for Technical Processes*, vol. 8, Mexico City, Mexico, 2012; 222–227.
19. Sontag ED, Wang Y. On characterizations of the input-to-state stability property. *Systems & Control Letters* 1995; **24**(5):351–359.
20. Jiang Z, Wang Y. Input-to-state stability for discrete-time nonlinear systems. *Automatica* 2001; **37**(6):857–869.
21. Sontag E. Input to state stability: Basic concepts and results. *Nonlinear and Optimal Control Theory* 2008; :163–220.
22. Lazar M, Heemels W. Global input-to-state stability and stabilization of discrete-time piecewise affine systems. *Nonlinear Analysis: Hybrid Systems* 2008; **2**(3):721–734.
23. Löfberg J. YALMIP : A toolbox for modeling and optimization in MATLAB. *Proceedings of the IEEE Conference on Computer Aided Control Systems Design*, 2004; 284–289.
24. Verdult V, Lovera M, Verhaegen M. Identification of linear parameter-varying state-space models with application to helicopter rotor dynamics. *International Journal of Control* 2004; **77**(13):1149–1159.
25. Tóth R. *Modeling and identification of linear parameter-varying systems*, vol. 403. Springer, 2010.
26. Prempain E, Postlethwaite I, Benchaib A. A linear parameter variant¡ i¿ h¡/i¿¡ sub¿¡/sub¿ control design for an induction motor. *Control Engineering Practice* 2002; **10**(6):633–644.

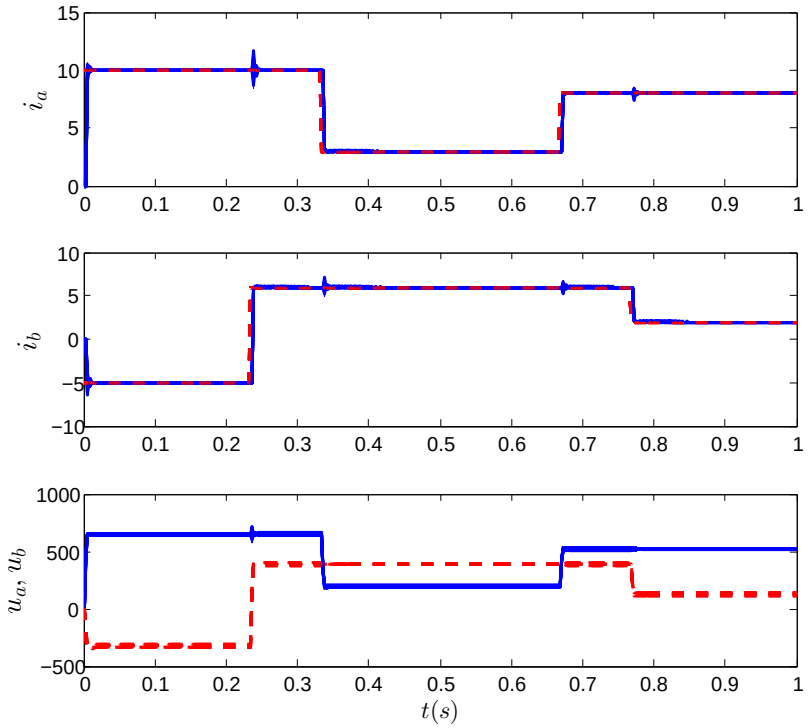

Figure 12. Simulation of the faulty system with a re-designed controller with 10 equally spaced values of ω in the range -110 to 110 subject to loss of measurement of i_b and 40% loss of actuator gains. Top: i_a, solid and i_{a_r} dashed, Middle: i_b, solid and i_{b_r} dashed, Bottom: u_a solid, u_b dashed.

A. PROOFS

A.1. Proof of Theorem 3

Consider

$$V(e(k)) = e(k)^T \mathbf{P}(k) e(k) \tag{51}$$

with $\mathbf{P}(k) = \sum_{i=1}^{N} p_i(k) P_i$ as the ISS Lyapunov function candidate. To prove the ISS of the system we use Theorem 1 and show that this candidate LF satisfies relations of the form (5) and (6).

The first step is to show that (51) satisfies a relation of the form (5). If (22) is satisfied then, we have:

$$\begin{bmatrix} -I & I \\ I & -P_i \end{bmatrix} < 0. \tag{52}$$

Using Schur complement, it implies that $P_i > I$. Also, (22) implies:

$$\begin{bmatrix} P_j - G_i - G_i^T & G_i \\ * & -\sigma_d I \end{bmatrix} < 0. \tag{53}$$

By Schur complement, this implies that $G_i + G_i^T - P_j > \sigma_d^{-1} G_i G_i^T > 0$. From the fact that $G_i P_j^{-1} G_i^T \geq G_i + G_i^T - P_j$, it follows that $G_i P_j^{-1} G_i^T > \sigma_d^{-1} G_i G_i^T$. Therefore, $P_j < \sigma_d I$, and we have $P_i > I$. Since $\sum_{i=1}^{N} p_i(k) = 1$, we have:

$$\|e(k)\|^2 \leq V(e(k)) \leq \sigma_d \|e(k)\|^2. \tag{54}$$

The second step is to show that the candidate LF satisfies a relation of the form (6). We use the relation $G_i P_j^{-1} G_i^T \geq G_i + G_i^T - P_j$ again which implies that feasibility of (22) is a sufficient condition

DOI: 10.1002/rnc

for the feasibility of the following matrix inequality:

$$\begin{bmatrix} -G_i P_j^{-1} G_i^T & 0 & G_i A_i + U_i C_f & G_i \\ * & -I & I & 0 \\ * & * & -P_i & 0 \\ * & * & * & -\sigma_d I \end{bmatrix} < 0 \; \forall i, j = 1, \cdots, N. \tag{55}$$

Pre- and post-multiplying the above inequality with $\text{diag}\{G_i^{-1}, I, I, I\}$ and its transpose and noting that $L_i = G_i^{-1} U_i$, we get:

$$\begin{bmatrix} -P_j^{-1} & 0 & A_i + L_i C_f & I \\ * & -I & I & 0 \\ * & * & -P_i & 0 \\ * & * & * & -\sigma_d I \end{bmatrix} < 0 \; \forall i, j = 1, \cdots, N, \tag{56}$$

Multiplying the above inequality by $p_i(k)$ for each i, j and summing them together over i for each j, and then multiplying the resulting N inequalities by $p_j(k+1)$ and summing them together, and finally applying the Schur complement we get:

$$\begin{bmatrix} -\sum_{i=1}^N p_i(k) P_i & 0 \\ 0 & -\sigma_d I \end{bmatrix} - \\ \begin{bmatrix} \sum_{i=1}^N p_i(k)(A_i + L_i C_f)^T & I \\ I & 0 \end{bmatrix} \begin{bmatrix} -\sum_{j=1}^N p_j(k+1) P_j & 0 \\ 0 & -I \end{bmatrix} \begin{bmatrix} \sum_{i=1}^N p_i(k)(A_i + L_i C_f) & I \\ I & 0 \end{bmatrix} < 0, \tag{57}$$

Define $A_\delta(k) = \sum_{i=1}^N p_i(k)(A_i + L_i C_f)$ and note that $\mathbf{P}(k) = \sum_{i=1}^N p_i(k) P_i$ and $\mathbf{P}(k+1) = \sum_{j=1}^N p_j(k+1) P_j$. Then, the above inequality is is equal to:

$$\begin{bmatrix} A_\delta(k)^T \mathbf{P}(k+1) A_\delta(k) - \mathbf{P}(k) + I & A_\delta(k)^T \mathbf{P}(k+1) \\ * & \mathbf{P}(k+1) - \sigma_d I \end{bmatrix} < 0 \tag{58}$$

Pre- and post-multiplying the above inequality with $\begin{bmatrix} e(k)^T & v(k)^T \end{bmatrix}^T$ and its transpose gives:

$$(A_\delta(k) e(k) + v(k))^T \mathbf{P}(k+1)(A_\delta(k) e(k) + v(k)) - e(k)^T \mathbf{P}(k) e(k) \leq \\ -e(k)^T e(k) + \sigma_d v(k)^T v(k). \tag{59}$$

The above inequality can be rewritten as:

$$(e(k+1))^T \mathbf{P}(k+1)(e(k+1)) - e(k)^T \mathbf{P}(k+1) e(k) \leq -e(k)^T e(k) + \sigma_d v(k)^T v(k), \tag{60}$$

which is:

$$V(e(k+1)) - V(e(k)) \leq -\|e(k)\|^2 + \sigma_d \|v(k)\|^2, \tag{61}$$

Therefore, based on Theorem 1, $V(e(k))$ is an ISS Lyapunov function for the error system and the error system is ISS with respect to $v = -B_d d$.

Now, we move to the calculation of the ISS gain. The inequality (61) together with (54) gives:

$$V(e(k+1)) \leq V(e(k))(1 - \frac{1}{\sigma_d}) + \sigma_d \|v(k)\|^2. \tag{62}$$

Applying (62) for $k = 0$ up to $k = \kappa$ in an inductive manner gives:

$$V(e(\kappa)) \leq V(e(0))(1 - \frac{1}{\sigma_d})^\kappa + \sigma_d \sum_{l=0}^{\kappa-1} \left(1 - \frac{1}{\sigma_d}\right)^{\kappa-l-1} \|v(l)\|^2 \\ \leq (1 - \frac{1}{\sigma_d})^\kappa V(e(0)) + \sigma_d^2 \|v\|_\infty^2. \tag{63}$$

DOI: 10.1002/rnc

Since from (54) $V(e(0)) \leq \sigma_d \|e(0)\|^2$, the above inequality implies:

$$\|e(\kappa)\| \leq \sqrt{\sigma_d}\left(1-\frac{1}{\sigma_d}\right)^{\kappa/2}\|e(0)\| + \sigma_d\|v\|_\infty. \tag{64}$$

This proves that the system is ISS with respect to v with the ISS gain $\gamma_v(s) = \sigma_d s, s \in \mathbb{R}_{\geq 0}$. Consequently, the ISS gain w.r.t. d is $\|B_d\|\sigma_d$.

A.2. Proof of Theorem 4

Consider

$$V(x_\Delta(k)) = x_\Delta(k)^T \mathbf{P}(k) x_\Delta(k), \tag{65}$$

where $\mathbf{P}(k) = \sum_{i=1}^N p_i(k) P_i$ with $P_i = Q_i^{-1}$ as a candidate LF for the difference system (19).

If (26) is feasible, then it holds that:

$$\begin{bmatrix} -I & Q_i \\ * & -Q_i \end{bmatrix} < 0, \tag{66}$$

which by using Schur complement implies that $Q_i^{-1} = P_i > I$. Also, we have that:

$$\begin{bmatrix} -Q_j & I \\ I & -\sigma_a I \end{bmatrix} < 0 \tag{67}$$

which yields $Q_j^{-1} = P_j \leq \sigma_a I$. Therefore, $V(x_\Delta)$ satisfies:

$$\|x_\Delta(k)\|^2 \leq V(x_\Delta(k)) \leq \sigma_a \|x_\Delta(k)\|^2. \tag{68}$$

Post- and pre-multiplying (26) by $\mathrm{diag}\{I, I, Q_i^{-1}, I\}$ and its transpose and using the relation $M_i = Y_i Q_i^{-1}$ we get:

$$\begin{bmatrix} -Q_j & 0 & A_i + B_f M_i & I \\ 0 & -I & I & 0 \\ * & * & -Q_i^{-1} & 0 \\ * & * & * & -\sigma_a I \end{bmatrix} < 0 \ \forall i, j = 1, \cdots, N. \tag{69}$$

Multiplying the above inequality by $p_i(k)$ for each i, j and summing them together over i for each j, and then multiplying the resulting N inequalities by $p_j(k+1)$ and adding them together, and finally by using the Schur complement we get:

$$\begin{bmatrix} \mathbf{P}(k) + I & 0 \\ * & -\sigma_a I \end{bmatrix} + \\ \begin{bmatrix} \sum_{i=1}^N p_i(k)(A_i + B_f M_i) & I \end{bmatrix}^T \begin{bmatrix} \mathbf{P}(k+1) \end{bmatrix} \begin{bmatrix} \sum_{i=1}^N p_i(k)(A_i + B_f M_i) & I \end{bmatrix} < 0, \tag{70}$$

where $\mathbf{P}(k+1) = \sum_{j=1}^N p_j(k+1) P_j$ with $P_j = Q_j^{-1}$ and $\mathbf{P}(k) = \sum_{i=1}^N p_i(k+1) P_i$ with $P_i = Q_i^{-1}$. Pre- and post-multiplying the above inequality with $\begin{bmatrix} x_\Delta(k)^T & w(k) \end{bmatrix}^T$ and its transpose and knowing that $x(k+1) = \sum_{i=1}^N (A_i + B_f M_i) x(k) + w(k)$ we get:

$$x(k+1)^T \mathbf{P}(k+1) x(k+1) - x(k) \mathbf{P}(k) x(k) \leq -x(k)^T x(k) + \sigma_a w(k)^T w(k). \tag{71}$$

which is

$$V(x_\Delta(k+1)) - V(x_\Delta(k)) \leq -\|x_\Delta(k)\|^2 + \sigma_a \|w(k)\|^2, \tag{72}$$

Therefore, based on Theorem 1 , the closed-loop system is ISS with respect to $w(k)$. The ISS gain is calculated using the same procedure as we used for the observation error system. The ISS gain

Prepared using rncauth.cls
DOI: 10.1002/rnc

with respect to w is $\gamma_w(s) = \sigma_w s$. To obtain the ISS gain w.r.t u_c and e, note that

$$w(k) = \begin{bmatrix} B_\Delta & -\sum_{i=1}^N p_i(k)(L_i C_f) \end{bmatrix} \begin{bmatrix} u_c(k) \\ e(k) \end{bmatrix}$$

Therefore, we have:

$$V(x_\Delta(k+1)) - V(x_\Delta(k)) \leq -\|x_\Delta(k)\|^2 + \sigma_a \|B_\Delta\|^2 \|u_c(k)\|^2 + \sigma_a c_1^2 \|C_f\|^2 \|e(k)\|^2, \quad (73)$$

where $c_1 = \max_{1\leq i\leq N} \|L_i\|$. Using the same procedure as in the proof of Theorem 3 we obtain that the ISS gain w.r.t. u_c is $\gamma_u(s) = \sigma_a \|B_\Delta\| s$ and ISS gain w.r.t. e is $\gamma_e(s) = \sigma_a c_1 \|C_f\| s$.

A.3. Proof of Lemma 1

Consider the following candidate LF:

$$V(e(k), x_\Delta(k)) = \mu V_e(e(k)) + V_\Delta(x_\Delta(k)), \quad (74)$$

with $\mu > 0$ for the interconnection where V_e is the LF in (51) and V_Δ is the LF in (65). From (61) and (73), we have

$$\begin{aligned} &V(x(k+1), e(k+1)) - V(x(k), e(k)) \leq \\ &-\mu \|e(k)\|^2 + \mu \sigma_d \|B_d\|^2 \|d(k)\|^2 - \|x_\Delta(k)\|^2 + \sigma_a \|B_\Delta\|^2 \|u_c(k)\|^2 + \sigma_a c_1^2 \|C_f\|^2 \|e(k)\|^2 \\ &= (\sigma_a c_1^2 \|C_f\|^2 - \mu) \|e(k)\|^2 + \mu \sigma_d \|B_d\|^2 \|d(k)\|^2 - \|x_\Delta(k)\|^2 + \sigma_a \|B_\Delta\|^2 \|u_c(k)\|^2. \end{aligned} \quad (75)$$

Denote $c_2 = \|B_d\|, c_3 = \|B_\Delta\|$. If we choose $\mu = \sigma_a c_1^2 \|C_f\|^2 + 1$, then we have:

$$\begin{aligned} &V(x(k+1), e(k+1)) - V(x(k), e(k)) \leq \\ &-\|e(k)\|^2 - \|x_\Delta(k)\|^2 + \mu \sigma_d c_2^2 \|d(k)\|^2 + \sigma_a c_3^2 \|u_c(k)\|^2 \leq \\ &-\| \begin{bmatrix} e(k) \\ x_\Delta(k) \end{bmatrix} \|^2 + \mu \sigma_d c_2^2 \|d(k)\|^2 + \sigma_a c_3^2 \|u_c(k)\|^2, \end{aligned} \quad (76)$$

which proves that the interconnection is ISS w.r.t d and u_c. The next step is to compute the ISS gains. From (54) and (68), we have:

$$\mu \|e(k)\|^2 + \|x_\Delta(k)\|^2 \leq V(k) \leq \mu \sigma_d \|e(k)\|^2 + \leq \sigma_a \|x_\Delta(k)\|^2. \quad (77)$$

Denote $c_4 = \max(\mu \sigma_d, \sigma_a)$, $e_r = \begin{bmatrix} e \\ x_\Delta \end{bmatrix}$ and note that $\mu = \sigma_a c_1^2 \|C_f\|^2 + 1 \geq 1$. Then we have:

$$\|e_r(k)\|^2 \leq V(e_r(k)) \leq c_4 \|e_r(k)\|^2. \quad (78)$$

The above inequality with (76) gives:

$$V(e_r(k+1)) \leq (1 - \frac{1}{c_4}) V(e_r(k)) + \mu \sigma_d c_2^2 \|d(k)\|^2 + \sigma_a c_3^2 \|u_c(k)\|^2. \quad (79)$$

Applying the above inequality for $k = 0$ to $k = \kappa$ gives:

$$\begin{aligned} &V(e_r(\kappa)) \leq \\ &(1 - \frac{1}{c_4})^\kappa V(e_r(0)) + \mu \sigma_d c_2^2 \sum_{l=0}^{\kappa-1} (1 - \frac{1}{c_4})^{\kappa-l-1} \|d(l)\|^2 + \sigma_a c_3^2 \sum_{l=0}^{\kappa-1} (1 - \frac{1}{c_4})^{\kappa-l-1} \|u_c(l)\|^2 \leq \\ &(1 - \frac{1}{c_4})^\kappa V(e_r(0)) + \mu \sigma_d c_2^2 c_4 \|d\|_\infty^2 + \sigma_a c_3^2 c_4 \|u_c\|_\infty^2. \end{aligned} \quad (80)$$

Since $V(e_r(0)) \leq c_4 \|e_r(0)\|^2$, the above inequality implies:

$$\|e_r(\kappa)\| \leq \sqrt{c_4} (1 - \frac{1}{c_4})^{\kappa/2} \|e_r(0)\| + c_2 \sqrt{\mu \sigma_d c_4} \|d\|_\infty + c_3 \sqrt{\sigma_a c_4} \|u_c\|_\infty. \quad (81)$$

Threfore, the ISS gain w.r.t. d is $c_2 \sqrt{\mu \sigma_d c_4} s$ and w.r.t u_c is $c_3 \sqrt{\sigma_a c_4} s$.

DOI: 10.1002/rnc

A.4. *Proof of Theorem 5*

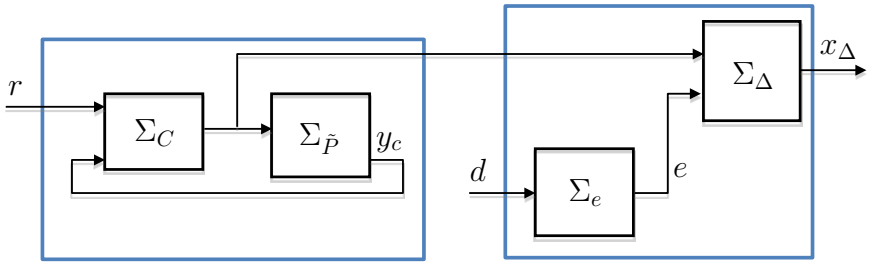

Figure 13. Closed-loop system as series connection of $(\Sigma_C, \Sigma_{\tilde{P}})$ and $(\Sigma_e, \Sigma_\Delta)$

To prove ISS of the closed-loop reconfigured system, we use Theorem 2 and the fact that the IOS of closed-loop system is equivalent to the IOS of the interconnection of the $(\Sigma_{\tilde{P}}, \Sigma_C)$ and $(\Sigma_e, \Sigma_\Delta)$ as shown in the Figure 13.

The closed-loop system that consists of the faulty system, the virtual sensor, the virtual actuator, and the nominal controller is given by:

$$\Sigma_{P_f} : \begin{cases} x_f(k+1) = A(\theta(k))x_f(k) + B_f u_f(k) + B_d d(k), \\ y_f(k) = C_f x_f(k), \end{cases} \tag{82a}$$

$$\Sigma_S : \hat{x}_f(k+1) = A_\delta(\theta)\hat{x}_f(k) + B_f u_c(k) - L(\theta)y_f(k), \tag{82b}$$

$$\Sigma_A : \begin{cases} \tilde{x}(k+1) = A(\theta)\tilde{x}(k) + Bu_c(k), \\ u_f(k) = -M(\theta)x_\Delta(k) - Ru_c(k), \\ y_c(t) = C\tilde{x}(k), \end{cases} \tag{82c}$$

$$\Sigma_C : \begin{cases} x_c(k+1) = f_c(x_c(k), y_c(k), r(k)) \\ u_c = h_c(x_c(k), y_c(k), r(k)) \end{cases} \tag{82d}$$

where x_c is the internal state of the controller. Using the change of the variables: $x_\Delta = \tilde{x} - \hat{x}_f$ and $e = \hat{x}_f - x_f$, we get:

$$\Sigma_{\tilde{P}} : \begin{cases} \tilde{x}(k+1) = A(\theta)\tilde{x}(k) + Bu_c(k), \\ y_c = C\tilde{x}_c, \end{cases} \tag{83a}$$

$$\Sigma_C : \begin{cases} x_c(k+1) = f_c(x_c(k), y_c(k), r(k)) \\ u_c = h_c(x_c(k), y_c(k), r(k)) \end{cases} \tag{83b}$$

$$\Sigma_e : e(k+1) = (A(\theta) + L(\theta)C_f)e(k) - B_d d(k) \tag{83c}$$

$$\Sigma_\Delta : x_\Delta(k+1) = (A(\theta) + B_f M(\theta))x_\Delta(k) + L(\theta)C_f e(k) + B_\Delta u_c(k), \tag{83d}$$

which is shown graphically in Figure (13). Since IOS properties are invariant under a linear change of variables ($y_f = C_f x_f, x_f = \tilde{x} - x_\Delta - e$), it is enough to show the IOS of (83).

The transformed system (83) consists of the cascade interconnection of the $(\Sigma_{\tilde{P}}, \Sigma_C)$ and $(\Sigma_e, \Sigma_\Delta)$ as shown in the Figure 13. Note that $\Sigma_{\tilde{P}}$ has the same dynamics as the nominal system Σ_P. Based on the assumption 1, we know that the nominal closed-loop system is IOS, therefore $(\Sigma_{\tilde{P}}, \Sigma_C)$ is also IOS and based on Theorems 3 and 4 Σ_e and Σ_Δ are ISS .

Moreover, in Lemma 1 we showed that the interconnection $(\Sigma_\Delta\ ,\ \Sigma_e)$ is ISS with respect to the inputs (u_c, d) and, therefore, it is IOS w.r.t the output (e, x_Δ). Based on Assumption 1, $(\Sigma_{\tilde{P}}, \Sigma_C)$ is IOS w.r.t to the input (r, d) and the output $(u_c, \tilde{x})$. Therefore, using Theorem 2 we conclude that the series connection $(\Sigma_{\tilde{P}}, \Sigma_C, \Sigma_e, \Sigma_\Delta)$ is IOS w.r.t to the input (r, d) and the output e, x_Δ, which proves the theorem.

DOI: 10.1002/rnc

A.5. Static Output Feedback Control Design for LPV systems

In this appendix, we give the details of design of an SOF controller for discrete time LPV systems. The structure and type of the controller is not important for our proposed method and is only given for the sake of completeness.

Consider an LPV system of the following form:

$$\Sigma_P : \begin{cases} x(k+1) = A(\theta(k))x(k) + Bu_c(k) + B_d d(k), \\ y(k) = Cx(k), \\ z(k) = C_z x(k) + D_z d(k), \end{cases} \tag{84}$$

where A is defined as in (9), z is the performance vector. The goal is to design a static output feedback controller of the form:

$$u(k) = K(\theta)y(k) = \sum_{i=1}^{N} p_i K_i y(k). \tag{85}$$

We assume without loss of generality that the output matrix is of full row rank. Then, there exist nonsingular transformation matrices T_C such that $CT_C = \begin{bmatrix} I & 0 \end{bmatrix}$. This transformation matrix is not unique for a given C. A special case is given by $T_C = \begin{bmatrix} C^T(CC^T)^{-1} & C^{\perp} \end{bmatrix}$ where $C^{\perp}$ is an orthogonal basis for the null space of C. We define the following matrices: $\tilde{A}_i = T_C A_i T_C$, $\tilde{B} = T_C^{-1}B$, $\tilde{C}_z = C_z T_C$, $\tilde{B}_d = T_C^{-1}B_d$.

Theorem 6

If there exist symmetric matrices $Q_i = Q_i^T$ and matrices $G_i = \begin{bmatrix} G_{11i} & 0 \\ G_{21i} & G_{22i} \end{bmatrix}$ such that:

$$\begin{bmatrix} -Q_j & 0 & \tilde{A}_i G_i + \tilde{B}\begin{bmatrix} U_i & 0 \end{bmatrix} & \tilde{B}_d \\ * & -I & \tilde{C}_z G_i & D_z \\ * & * & Q_i - G_i - G_i^T & 0 \\ * & * & * & -\gamma I \end{bmatrix} < 0 \; \forall \, i, j = 1, \cdots, N, \tag{86}$$

then, the LPV system (84) is stable with the H_∞ performance index $\sqrt{\gamma}$ i.e. $\sum_{k=0}^{\infty}\|z(k)^2\| < \gamma \sum_{k=0}^{\infty}\|d(k)\|^2$. The controller gains K_i are given by:

$$K_i = U_i G_{11i}^{-1}. \tag{87}$$

Proof

Denote $Q_i = T_C \tilde{Q}_i T_C^T$, then $\tilde{Q}_i = T_C^{-1} Q_i T_C^{-T}$. Therefore, (86) is equal to:

$$\begin{bmatrix} -T_C^{-1}Q_j T_C^{-T} & 0 & T_C^{-1}A_i T_C G_i + T_C^{-1}B\begin{bmatrix} U_i & 0 \end{bmatrix} & T_C^{-1}B_d \\ * & -I & C_z T_C G_i & D_{zi} \\ * & * & T_C^{-1}Q_i T_C^{-T} - G_i - G_i^T & 0 \\ * & * & * & -\gamma I \end{bmatrix} < 0, \; \forall i, j = 1, \ldots, N. \tag{88}$$

Pre- and post multiplying the above inequality by: $\mathrm{diag}\{\begin{bmatrix} T_C & I & T_C & I \end{bmatrix}\}$ and its transpose, and denoting $\tilde{G}_i = T_C G_i T_C^T$ we get:

$$\begin{bmatrix} -Q_j & 0 & A_i \tilde{G}_i + B\begin{bmatrix} U_i & 0 \end{bmatrix} T_C^T & B_d \\ * & -I & C_z \tilde{G}_i & D_z \\ * & * & Q_i - \tilde{G}_i - \tilde{G}_i^T & 0 \\ * & * & * & -\gamma I \end{bmatrix} < 0 \;\; \forall i, j = 1, \ldots, N. \tag{89}$$

Since $K_i = U_i G_{11i}^{-1}$, using the structure of G_i, we have:

$$\begin{bmatrix} U_i & 0 \end{bmatrix} = K_i \begin{bmatrix} I & 0 \end{bmatrix} \begin{bmatrix} G_{11_i} & 0 \\ G_{21_i} & G_{22_i} \end{bmatrix}.$$

DOI: 10.1002/rnc

Substituting $\begin{bmatrix} I & 0 \end{bmatrix}$ with CT_C, then: $\begin{bmatrix} U_i & 0 \end{bmatrix} = K_i CT_C G_i$. Therefore, (89) is equal to

$$\begin{bmatrix} -Q_j^T & 0 & A_i\tilde{G}_i + BK_i\tilde{G}_i & B_d \\ * & -I & C_{zi}\tilde{G}_i & D_z \\ * & * & Q_i - \tilde{G}_i - \tilde{G}_i^T & 0 \\ * & * & * & -\gamma I \end{bmatrix} < 0 \ \forall i, j = 1, \ldots, N \tag{90}$$

Using the fact $Q_i - \tilde{G}_i - \tilde{G}_i^T \geq -\tilde{G}_i Q_i^{-1} \tilde{G}_i^T$ and by pre- and post-multiply the above inequality with $diag\{\begin{bmatrix} I & I & \tilde{G}_i^{-1} & I \end{bmatrix}\}$ and its transpose, we find that if the above inequality is satisfied, then we have:

$$\begin{bmatrix} -Q_j & 0 & A_i + BK_i C & B_d \\ * & -I & C_z & D_z \\ * & * & -Q_i^{-1} & 0 \\ * & * & * & -\gamma I \end{bmatrix} < 0 \ \forall i, j \in 1, \ldots, N. \tag{91}$$

The rest of the proof is easily followed using the same pattern as in the proof of Theorem 3 or 4 and is omitted here for the sake of space. □

DOI: 10.1002/rnc